High-order classical adiabatic reaction forces: slow manifold for a spin model

2010 J. Phys. A: Math. Theor. 43 045102

(http://iopscience.iop.org/1751-8121/43/4/045102)

IOP PUBLISHING JOURNAL OF PHYSICS A: MATHEMATICAL AND THEORETICAL

J. Phys. A: Math. Theor. **43** (2010) 045102 (27pp) doi:10.1088/1751-8113/43/4/045102

High-order classical adiabatic reaction forces: slow manifold for a spin model

M V Berry[1] **and P Shukla**[2]

[1] H H Wills Physics Laboratory, Tyndall Avenue, Bristol BS8 1TL, UK
[2] Department of Physics, Indian Institute of Technology, Kharagpur, India

Received 11 September 2009
Published 8 January 2010
Online at stacks.iop.org/JPhysA/43/045102

Abstract

The influence of a fast system on the hamiltonian dynamics of a slow system coupled to it is explored by calculating, in a model, high-order smooth (nonoscillating) adiabatic reaction forces (i.e. beyond Born–Oppenheimer and geometric magnetism). The model is a spin (fast) driven by, and reacting on, the position vector (slow) of a particle coupled to it. The search for smooth solutions is equivalent to determining the slow manifold in the full phase space, on which, in the model system, the spin would not precess. The series of reactions for the nonlinear coupled system diverges factorially, as in the simpler linear case of a spin being driven passively by a position vector changing in a prescribed manner. When the particle is closest to the origin, all terms in the divergent series have the same sign, indicating a Stokes phenomenon and suggesting that a solution of the slow manifold equation exists but contains exponentially weak precession oscillations. The predicted oscillations are observed numerically, and shown to be inevitable for the exactly solvable linearized slow manifold which is equivalent to the Landau–Majorana–Zener model of quantum mechanics.

PACS numbers: 03.65.Vf, 02.30.Mv, 02.40.Yy, 45.50.Dd

1. Introduction

For classical or quantum systems consisting of interacting components with very different time scales, it is natural to seek an adiabatic description, in which the fast and slow dynamics are separated [1]. Examples are the Born–Oppenheimer separation of electronic (fast) and nuclear (slow) motion in the quantum physics of molecules [2, 3], and the determination of slow manifolds in classical dynamics [4, 5]. In leading order (Born–Oppenheimer approximation), the slow variables are regarded as frozen parameters affecting the fast variables, whose average motion in turn affects the slow dynamics. To the next order, the slow velocity provides a correction to the fast dynamics, in the form of the geometric phase (quantum [6, 7]) or the

Hannay angle (classical [8]); the reaction of these geometric phenomena on the slow dynamics takes the form of a 'geometric magnetic' force [9, 10].

Higher-order corrections to the fast dynamics imply higher-order reactions on the slow dynamics. Our purpose here is to investigate these higher-order reaction forces in the simplest case, where the dynamics is classical, hamiltonian and nonresonant. Previous studies have identified several forces beyond geometric magnetism: an 'electric' force [9, 11], the Littlejohn–Weigert (LJ) force [12] and, in chaotic fast systems, deterministic friction [13, 14] and the Jarzynski force [14]. Studies of high orders of an expansion in the slowness parameter have been envisaged [4, 15], and different resummation schemes have been compared [16] but not carried out in explicit detail. The general case seems complicated, but by making several simplifications we are able to study high-order post-geometric reactions and make progress in understanding their asymptotics.

The study of adiabatic reaction forces in the coupled problem is more difficult than determining the fast motion when slaved to (i.e. driven by) slow variables with prescribed time-dependence. In the slaved problem, the high-order fast motion depends on high time derivatives of the slow variables. When inserted naively into formulas for the reaction forces on the slow system, this would give slow accelerations depending on time derivatives higher than the second, and hence, in the coupled problem, slow equations of motion with many redundant solutions. To avoid this, and determine high-order reaction forces correctly, it is necessary to employ a self-consistent procedure.

The central simplification is to consider not the most general motion, which would involve averaging over the fast oscillations [17] that are weakly inherited by the slow motion. Instead, we restrict attention to certain special motions, in which the fast oscillations are suppressed by studying perturbations of an equilibrium configuration for fixed slow variables, and seek fast solutions clinging as closely as possible to the slow variables when these are freed to change. In dynamical systems terminology, this is the slow manifold, to which motion in the full slow-fast phase space is restricted by choosing the special fast motions. (There are analogues of the slow manifolds, associated with periodic orbits rather than equilibrium configurations [4], but, consistent with our decision to study only the simplest situation, we do not consider these further.)

To proceed further, a model system is introduced (section 2), consisting of a heavy spinning particle moving in three dimensions, with the spin precessing rapidly about the particle's position vector, to which it is strongly coupled and upon which it reacts. The fast system is the spin, and the position and conjugate momentum of the particle constitute the slow system. Previously [10], it was shown for this model that the geometric magnetic and electric reaction forces describe qualitatively distinct features of the exact motion. Appendix A describes a slight generalization of the spin model, in which the fast motion is an arbitrary hamiltonian system rather than a spin; an instructive calculation demonstrates the geometric magnetic correction to the Born–Oppenheimer force. Further generalizations have been studied, in quantum as well as classical mechanics, in which the fast dynamics is coupled to the slow momenta as well as the position [18–21], but the position-dependent spin model is sufficient for our study of high-order reactions. A technical aspect of the spin model is elaborated in appendix B.

An exact nonlinear self-consistent formalism for the slow manifold is developed in section 3, leading to an equation that in principle would determine it. The slow manifold equation is used to generate recurrence relations for the adiabatic series of reaction forces, and the first four are determined explicitly. The first three illustrate previously derived general forces: the Born–Oppenheimer, geometric magnetic [10] and Littlejohn–Weigert ([12] and appendix C) forces. The fourth is new.

Section 4 is devoted to the regime in which the slow manifold equation can be approximated by its linearization. The first three corresponding adiabatic reaction forces agree with those in the nonlinear theory, but the fourth and higher are different. The linearized equation is solved exactly, using its equivalence to the Landau–Majorana–Zener [22–24] model familiar in the quantum mechanics of a slaved spin. The resulting exact linear slow manifold possesses exponentially weak oscillations in addition to the smooth adiabatic reactions. The oscillations are associated with the Stokes phenomenon of asymptotics, and reflect the divergence of the series of reactions, associated with nonadiabatic effects when the particle is closest to the origin.

Section 5 is numerical. Trajectory computations for the full coupled dynamics show how the precession gets increasingly suppressed as more reaction forces are included and the spin clings more closely to the slow manifold. But the linear theory strongly suggests that weak oscillations are inevitable in the nonlinear manifold too, and will appear when the particle's distance from the origin is a minimum; this too is demonstrated numerically.

Section 6 is an exploration of the high orders of the series of reaction forces, as functions on the slow phase space. A combined analytical and numerical approach indicates that, as in the linear theory, the series diverges factorially in the manner familiar in asymptotics. The situation corresponding to the Stokes phenomenon, indicating the birth of exponentially weak oscillations, is where the divergent terms all have the same sign. We show that this corresponds to orthogonality of the particle's position and velocity vectors and the distance from the origin being a minimum.

This study suggests the conclusion (section 7) that a slow manifold exists, in the sense of an exact solution of the slow manifold equation of section 3. But although this represents solutions in which the spin and the particle are forever locked together, the fast oscillations have not been completely suppressed: they persist, albeit exponentially weakly. Therefore 'slow manifold' might not be the best terminology; but it is well established, so we continue to use it ('Slaved manifold' might be more accurate).

While writing this paper, we learned of a recent work by Vanneste [25], concerning a different system but taking a similar approach to the study of the slow manifold via the high orders of the adiabatic expansion.

2. Spin model

The position $\boldsymbol{R} = \{X, Y, Z\}$ of a heavy particle with momentum $\boldsymbol{P} = \{P_X, P_Y, P_Z\}$ is strongly coupled to its classical spin $\boldsymbol{S}$, according to the hamiltonian [10, 12, 26]

$$H = \frac{1}{2}\varepsilon \boldsymbol{P}\cdot\boldsymbol{P} + \frac{1}{\varepsilon}\boldsymbol{R}\cdot\boldsymbol{S}, \tag{2.1}$$

in which ε is the small slowness parameter. Thus $\boldsymbol{R}$ acts as a 'magnetic field', dipole-coupled to $\boldsymbol{S}$. Fancifully, this could represent a large homogeneous sphere of 'monopolium', inside which the spinning particle is moving without resistance; alternatively, it could represent a thin spinning molecule with an axial electric dipole moment, moving through a uniformly charged sphere. The slow dynamics is determined by

$$\dot{\boldsymbol{R}} \equiv \boldsymbol{V} = \nabla_{\boldsymbol{P}} H = \varepsilon \boldsymbol{P}, \qquad \dot{\boldsymbol{P}} = \frac{\dot{\boldsymbol{V}}}{\varepsilon} = -\nabla_{\boldsymbol{R}} H = -\frac{1}{\varepsilon}\boldsymbol{S}, \tag{2.2}$$

so the force on the particle is

$$\boldsymbol{F} = \ddot{\boldsymbol{R}} = \dot{\boldsymbol{V}} = -\boldsymbol{S}. \tag{2.3}$$

For the fast dynamics, we use the fact that the spin can be regarded as a hamiltonian system with one degree of freedom, where the two-dimensional phase space is a sphere whose

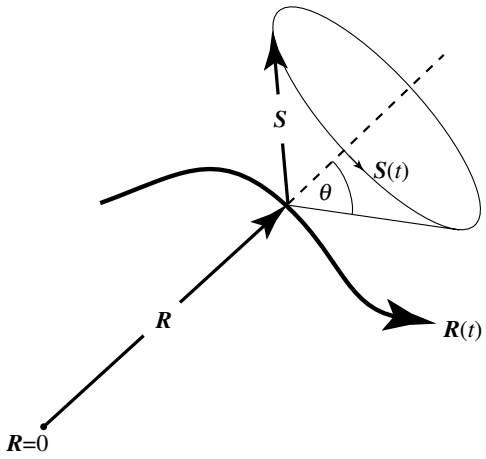

Figure 1. Spin $\boldsymbol{S}$ precessing about the instantaneous position vector $\boldsymbol{R}$.

azimuth angle about any axis is the coordinate q and where the component of spin along that axis is the conjugate momentum p. The resulting Hamilton equations give

$$\dot{\boldsymbol{S}} = \frac{1}{\varepsilon}\boldsymbol{R} \times \boldsymbol{S}, \tag{2.4}$$

describing precession of $\boldsymbol{S}$ about the instantaneous position $\boldsymbol{R}$, with angular velocity R/ε (figure 1). If the position $\boldsymbol{R}(t)$ were a prescribed function of time, rather than being determined dynamically by (2.3), the precession equation (2.4) would determine the dynamics of the slaved spin.

This spin equation automatically preserves the magnitude $|\boldsymbol{S}|$ of the spin. In addition, rotational invariance leads to the conservation of the total angular momentum (orbital + spin), that is

$$\boldsymbol{J} = \frac{1}{\varepsilon}\boldsymbol{R} \times \boldsymbol{V} + \boldsymbol{S} = \text{constant}, \tag{2.5}$$

and it is easily confirmed that this follows from the equations of motion (2.3) and (2.4). Of course the total energy $E = H$ is conserved too.

We note immediately that conservation of $\boldsymbol{J}$ enables $\boldsymbol{S}$ to be eliminated, giving an equation for the slow dynamics alone: from (2.3),

$$\boldsymbol{F} = \dot{\boldsymbol{V}} = \frac{1}{\varepsilon}\boldsymbol{R} \times \boldsymbol{V} - \boldsymbol{J} = \boldsymbol{R} \times \boldsymbol{P} - \boldsymbol{J}. \tag{2.6}$$

This reduced dynamics, of the slow system with three freedoms, corresponds to a particle moving in a uniform 'gravitational' field $-\boldsymbol{J}$ and, again, the magnetic field $-\boldsymbol{R}$ of a sphere of monopolium. This magnetic field is not divergenceless, so there is no corresponding vector potential and it might seem that the slow dynamics (2.6) is not hamiltonian. However, an argument of Littlejohn and Weigert [12] (a special case of dynamical reduction [27]) shows that the three-freedom dynamics incorporating $\boldsymbol{J} =$ constant can be written in hamiltonian form for a system with two freedoms. Athough we will not make use of this fact, a slightly more explicit version of their argument is given in appendix B for completeness.

Equation (2.6) will be used in numerical computations of the slow dynamics, with $\boldsymbol{J}$ fixed by the initial conditions for $\boldsymbol{R}$, $\boldsymbol{V}$, and $\boldsymbol{S}$. But it does not generate the clinging solutions we are seeking, which correspond to particular initial conditions depending on $\boldsymbol{J}$. Therefore the

slow manifold does not correspond to a single value of $\boldsymbol{J}$; different trajectories on the slow manifold corrrespond to different $\boldsymbol{J}$. We specify the slow manifold in the next section.

We note that the parameter ε, and the magnitude $|\boldsymbol{S}|$ of the spin, can be eliminated from the equations of motion (2.3) and (2.4) by the scalings

$$\boldsymbol{R} \to \varepsilon^{2/3}|\boldsymbol{S}|^{1/3}\boldsymbol{R}, \qquad t \to \varepsilon^{1/3}|\boldsymbol{S}|^{-1/3}t. \tag{2.7}$$

Therefore small values of the slowness parameter ε correspond to the particle far from the origin (large R) and long times. The corresponding speed scaling is

$$V = |\boldsymbol{V}| \sim \varepsilon^{1/3} \sim R^{1/2}. \tag{2.8}$$

Nevertheless, in subsequent analysis it will be convenient to retain ε and $|\boldsymbol{S}|$; in numerical computations we will always choose $|\boldsymbol{S}| = 1$.

3. Slow manifold: where S clings to R

As in the previous section, the spin dynamics determined by (2.4) is non-precessing in lowest order if the spin is parallel or antiparallel to $\boldsymbol{R}$. For the coupled dynamics we are considering, it is necessary to distinguish the two cases: there are two slow manifolds. The following notation is convenient:

$$S = \pm\,|\boldsymbol{S}|\,. \tag{3.1}$$

Thus the lowest-order spin is

$$\boldsymbol{S}_0(\boldsymbol{R}) = S\boldsymbol{e}_R. \tag{3.2}$$

This is the lowest-order slow manifold, corresponding to the Born–Oppenheimer reaction force $-\boldsymbol{S}_0(\boldsymbol{R})$ on the slow particle according to (2.3). Thus the positive sign in (3.1) corresponds to a force attracting the particle to the origin, and the minus sign represents repulsion.

Beyond the lowest order, the clinging spin will depend on the particle velocity as well as its position. Thus we seek the slow manifold in the form $\boldsymbol{S}(\boldsymbol{R}, \boldsymbol{V})$. To find the equation this must satisfy, we note that the slow manifold is a particular invariant manifold, and differentiate with respect to time, using (2.3):

$$\dot{\boldsymbol{S}} = \dot{\boldsymbol{R}}\cdot\nabla_{\boldsymbol{R}}\boldsymbol{S} + \dot{\boldsymbol{V}}\cdot\nabla_{\boldsymbol{V}}\boldsymbol{S} = \boldsymbol{V}\cdot\nabla_{\boldsymbol{R}}\boldsymbol{S} - \boldsymbol{S}\cdot\nabla_{\boldsymbol{V}}\boldsymbol{S}. \tag{3.3}$$

Incorporating (2.4) gives the equation satisfied by $\boldsymbol{S}(\boldsymbol{R}, \boldsymbol{V})$:

$$\boldsymbol{V}\cdot\nabla_{\boldsymbol{R}}\boldsymbol{S} - \boldsymbol{S}\cdot\nabla_{\boldsymbol{V}}\boldsymbol{S} = \frac{1}{\varepsilon}\boldsymbol{R}\times\boldsymbol{S}. \tag{3.4}$$

This nonlinear partial differential equation is satisfied by any invariant manifold. For example, motivated by (2.5) we find that

$$\boldsymbol{S}(\boldsymbol{R}, \boldsymbol{V}) = -\frac{1}{\varepsilon}\boldsymbol{R}\times\boldsymbol{V} + \boldsymbol{J} \tag{3.5}$$

is a solution for any constant vector $\boldsymbol{J}$. But these do not include the manifold we seek, because, although $\boldsymbol{J}$ is conserved exactly along any trajectory, the slow manifold intersects (is foliated by) the solutions (3.5) for different $\boldsymbol{J}$.

To specify the slow manifold, we demand that $\boldsymbol{S}$ reduces to the Born–Oppenheimer force (3.2) when $\varepsilon \to 0$ for fixed $\boldsymbol{R}$ and $\boldsymbol{V}$ (excluding $\boldsymbol{R} = 0$), or equivalently, as $R \to \infty$ for fixed ε. But this is not quite enough, as experience with the linearized slow manifold (see section 4) indicates. An additional boundary condition is a consequence of the fact that the dynamical equations (2.2)–(2.4) guarantee that if the $\boldsymbol{S}$, $\boldsymbol{V}$ and $\boldsymbol{R}$ are initially parallel they will remain

so: the particle will move with constant acceleration on a line through the origin. Therefore we seek the solutions satisfying the boundary condition

$$\boldsymbol{S}((\boldsymbol{R}\cdot\boldsymbol{e}_V)\,\boldsymbol{e}_V,\boldsymbol{V}) = S\boldsymbol{e}_V. \tag{3.6}$$

Note that this differs from the superficially similar lowest-order adiabatic spin (3.2) in a crucial respect, that will have important implications later: in (3.2) the spin always points towards or away from the origin, and so reverses on a path through the origin, whereas (3.6) requires the spin to remain constant through the origin.

The solution $\boldsymbol{S}(t)$ of (3.4) and (3.6), with (3.2) as its large R asymptotics, is the slow manifold. We will also refer to it as the spin field in the slow phase space, or as the reaction force on the slow system (because of (2.3)).

To find a solution as an adiabatic series, we write

$$\boldsymbol{S}(\boldsymbol{R},\boldsymbol{V}) = \sum_{n=0}^{\infty}\varepsilon^n\boldsymbol{S}_n(\boldsymbol{R},\boldsymbol{V}), \tag{3.7}$$

in which $\boldsymbol{S}_0$ is independent of $\boldsymbol{V}$ and given by (3.2). Truncating the series at the term $n=N$ defines the Nth order slow manifold. Identifying powers of ε leads to

$$\boldsymbol{e}_R\times\boldsymbol{S}_0 = 0, \qquad \boldsymbol{e}_R\times\boldsymbol{S}_{n+1} = \frac{1}{R}\left(\boldsymbol{V}\cdot\nabla_{\boldsymbol{R}}\boldsymbol{S}_n - \sum_{l=0}^{n}\boldsymbol{S}_{n-l}\cdot\nabla_V\boldsymbol{S}_l\right). \tag{3.8}$$

This determines the components of $\boldsymbol{S}$ perpendicular to $\boldsymbol{R}$, which we separate by defining

$$\boldsymbol{S}_n = S_{n\parallel}\boldsymbol{e}_R + \boldsymbol{S}_{n\perp}, \qquad \text{i.e.} \quad S_{n\parallel} = \boldsymbol{S}_n\cdot\boldsymbol{e}_R. \tag{3.9}$$

Thus, from (3.8), after separating the $l=n$ term on the r.h.s using (3.2),

$$\boldsymbol{S}_{n+1\perp} = \frac{1}{R}\boldsymbol{e}_R\times\left(-\boldsymbol{V}\cdot\nabla_{\boldsymbol{R}}\boldsymbol{S}_n + S\boldsymbol{e}_R\cdot\nabla_V\boldsymbol{S}_n + \sum_{l=1}^{n-1}\boldsymbol{S}_{n-l}\cdot\nabla_V\boldsymbol{S}_l\right). \tag{3.10}$$

For the parallel components, we use

$$\begin{aligned} S^2 = \boldsymbol{S}\cdot\boldsymbol{S} &= \left(S\boldsymbol{e}_R + \sum_{n=1}^{\infty}\boldsymbol{S}_n\varepsilon^n\right)\cdot\left(S\boldsymbol{e}_R + \sum_{n=1}^{\infty}\boldsymbol{S}_n\varepsilon^n\right) \\ &= S^2 + 2S\sum_{n=1}^{\infty}\boldsymbol{e}_R\cdot\boldsymbol{S}_n\varepsilon^n + \sum_{n=2}^{\infty}\varepsilon^n\sum_{l=1}^{n-1}\boldsymbol{S}_{n-l}\cdot\boldsymbol{S}_l, \end{aligned} \tag{3.11}$$

whence

$$S_{n\parallel} = -\frac{1}{2S}\sum_{l=1}^{n-1}\boldsymbol{S}_{n-l}\cdot\boldsymbol{S}_l. \tag{3.12}$$

From this iteration scheme, we find the first four contributions to the slow manifold:

$$\begin{aligned} &\boldsymbol{S}_0 = S\boldsymbol{e}_R, \qquad \boldsymbol{S}_1 = \frac{S}{R^2}(\boldsymbol{V}\times\boldsymbol{e}_R), \qquad \boldsymbol{S}_2 = \frac{S}{R^4}\left(-\frac{1}{2}V_\perp^2\boldsymbol{e}_R + 3V_\parallel\boldsymbol{V}_\perp\right) \\ &\boldsymbol{S}_3 = \left(\frac{S}{2R^6}\left(30V_\parallel^2 - 5V_\perp^2\right) + 2\frac{S^2}{R^5}\right)\boldsymbol{e}_R\times\boldsymbol{V}. \end{aligned} \tag{3.13}$$

Here the velocity has been separated into components along and perpendicular to $\boldsymbol{R}$, i.e. $V = V_\parallel\boldsymbol{e}_R + \boldsymbol{V}_\perp$. The velocity-dependent force $-\varepsilon\boldsymbol{S}_1$ is geometric magnetism: a force of Lorentz type, generated by the magnetic field of a monopole with strength $-S$, which is the known form of the geometric magnetic field (2.19) for spin [9, 10]. As shown in appendix C,

$-\varepsilon^2 \boldsymbol{S}_2$ is the force identified by Littlejohn and Weigert [12]. Note that $-\varepsilon^3 \boldsymbol{S}_3$ is the first reaction force containing terms involving both S and S^2, because this is the first force influenced by the nonlinearity of (3.4). The electric reaction force [9] does not appear in the series, because it is proportional to the lowest-order spin component perpendicular to $\boldsymbol{R}$, which vanishes for the slow-manifold motions we are studying.

4. Linearized slow manifold

For large V, it is reasonable to regard the second term on the l.h.s. of (3.4) as small in comparison with the first, and study the linearized spin field equation

$$V \cdot \nabla_{\boldsymbol{R}} \boldsymbol{S} = \frac{1}{\varepsilon} \boldsymbol{R} \times \boldsymbol{S}. \tag{4.1}$$

A reason for studying this linearization is that it can be solved exactly and the corresponding slow manifold studied in detail. Since $\boldsymbol{V}$ appears simply as a parameter (there is no derivative involving $\boldsymbol{V}$ as in the full equation (3.4)), we can choose this vector to lie in any direction, e.g. along $\boldsymbol{e}_Z$. Thus

$$V \partial_Z \boldsymbol{S} = \frac{1}{\varepsilon} \boldsymbol{R} \times \boldsymbol{S}, \tag{4.2}$$

This preserves normalization, so we can choose the convention

$$\boldsymbol{S} \cdot \boldsymbol{S} = 1. \tag{4.3}$$

The boundary condition (3.6) becomes

$$\boldsymbol{S}(Z\boldsymbol{e}_Z, V\boldsymbol{e}_Z) = S\boldsymbol{e}_Z, \tag{4.4}$$

where $S = \pm 1$. Since the only variable is Z, we can regard X and Y as parameters, and without loss of generality exploit overall rotation symmetry and set $Y = 0$. Thus

$$\boldsymbol{R} = X\boldsymbol{e}_X + Z\boldsymbol{e}_Z \tag{4.5}$$

and (4.2) becomes

$$\begin{aligned} V\partial_Z S_X &= -\frac{ZS_Y}{\varepsilon} \\ V\partial_Z S_Y &= \frac{(ZS_X - XS_Z)}{\varepsilon} \\ V\partial_Z S_Z &= \frac{XS_Y}{\varepsilon}. \end{aligned} \tag{4.6}$$

The boundary condition (4.4) now corresponds to setting $X = 0$, and it is easy to see that (4.4) is a solution.

Before solving these linearized equations exactly, we need to establish compatibility with the adiabatic reactions (3.13) associated with the exact nonlinear dynamics. As in the nonlinear case, we separate parallel and perpendicular components (cf 3.9), and use (4.2) and the fact that $\boldsymbol{S} \cdot \boldsymbol{S} = 1$. This gives the recurrences

$$S_{n\parallel} = -\frac{1}{2} \sum_{m=1}^{n-1} \boldsymbol{S}_{n-m} \cdot \boldsymbol{S}_m, \qquad \boldsymbol{S}_{n+1\perp} = -\frac{V}{R} \boldsymbol{e}_R \times \partial_Z \boldsymbol{S}_n, \tag{4.7}$$

starting from

$$\boldsymbol{S}_0 = \boldsymbol{e}_R = \frac{X\boldsymbol{e}_X + Z\boldsymbol{e}_Z}{R} = \frac{X\boldsymbol{e}_X + Z\boldsymbol{e}_Z}{\sqrt{X^2 + Z^2}}. \tag{4.8}$$

Iteration leads to

$$\boldsymbol{S}_0 = \boldsymbol{e}_R, \qquad \boldsymbol{S}_1 = \frac{VX}{R^3}\boldsymbol{e}_Y, \qquad \boldsymbol{S}_2 = \frac{V^2X}{R^7}\left[-\left(\frac{1}{2}X^2 + 3Z^2\right)\boldsymbol{e}_X + \frac{5}{2}XZ\boldsymbol{e}_Z\right],$$
$$\boldsymbol{S}_3 = \frac{V^3X}{2R^{11}}(5X^4 - 25XZ^3 - 30X^4)\boldsymbol{e}_Y. \tag{4.10}$$

To compare these with the first four nonlinear spin fields (3.13), we use

$$\boldsymbol{V} = V\boldsymbol{e}_Z, \qquad V_\parallel = \boldsymbol{V}\cdot\boldsymbol{e}_R = \frac{VZ}{R}, \qquad \boldsymbol{V}_\perp = \boldsymbol{V} - V_\parallel\boldsymbol{e}_R = \frac{V}{R^2}(-XZ\boldsymbol{e}_X + X^2\boldsymbol{e}_Z), \tag{4.11}$$

and substitute into (3.13). This shows, after a little calculation, that the reaction forces $\boldsymbol{S}_0$, $\boldsymbol{S}_1$, and $\boldsymbol{S}_2$ (Born–Oppenheimer, geometric magnetism and Littlejohn–Weigert) are perfectly reproduced by the linearization. In $\boldsymbol{S}_3$ the only difference is that the term $2S^2/R^5$ in (3.13) is missing in (4.10). This is not surprising, because this is the first term that is not of order V^n; in fact it is of order V rather than V^3: it is the first term that reflects the nonlinearity. More generally, linearization will reproduce the terms of order V^n in all the forces $\boldsymbol{S}_n$.

To get an exact solution of the linearized equations, we transform the classical (4.6) to a form reminiscent of quantum mechanics, using

$$\boldsymbol{S} = \langle\psi|\boldsymbol{\sigma}|\psi\rangle = \{2\,\mathrm{Re}\,u * v, 2\,\mathrm{Im}\,u * v, |u|^2 - |v|^2\}, \tag{4.12}$$

in which $\boldsymbol{\sigma}$ is the vector of Pauli matrices, namely

$$\boldsymbol{\sigma} = \{\sigma_1, \sigma_2, \sigma_3\} = \left\{\begin{pmatrix}0 & 1\\ 1 & 0\end{pmatrix}, \begin{pmatrix}0 & -\mathrm{i}\\ \mathrm{i} & 0\end{pmatrix}, \begin{pmatrix}1 & 0\\ 0 & -1\end{pmatrix}\right\}, \tag{4.13}$$

and the 2-spinor

$$|\psi\rangle = \begin{pmatrix}u\\ v\end{pmatrix} \tag{4.14}$$

satisfies the 'Schrödinger lookalike' equation

$$\mathrm{i}\delta\partial_Z|\psi\rangle = -\frac{1}{2}\begin{pmatrix}Z & X\\ X & -Z\end{pmatrix}|\psi\rangle, \tag{4.15}$$

and in which we have written $\delta = \varepsilon V$. It is easy to confirm that normalization of $\langle\psi \mid \psi\rangle = 1$ implies the normalization (4.3).

Equation (4.15) is formally identical with the Landau–Majorana–Zener model [22–24] for a quantum spin 1/2 slaved to a changing magnetic field, in which the coordinate Z is replaced by time. An exact normalized solution, in terms of parabolic cylinder functions [28], is

$$\begin{pmatrix}u(X,Z,\delta)\\ v(X,Z,\delta)\end{pmatrix} = \exp\left(-\frac{\pi X^2}{16\delta}\right)\begin{pmatrix}X\sqrt{\frac{\mathrm{i}}{4\delta}}D_{-\frac{\mathrm{i}X^2}{4\delta}-1}\left(\frac{Z}{\sqrt{\delta}}\exp\left(-\frac{3}{4}\mathrm{i}\pi\right)\right)\\ D_{-\frac{\mathrm{i}X^2}{4\delta}}\left(\frac{Z}{\sqrt{\delta}}\exp\left(-\frac{3}{4}\mathrm{i}\pi\right)\right)\end{pmatrix}. \tag{4.16}$$

This satisfies the boundary condition, as can be seen from

$$\begin{pmatrix}u(0,Z,\delta)\\ v(0,Z,\delta)\end{pmatrix} = \begin{pmatrix}0\\ D_0\left(\frac{Z}{\sqrt{\delta}}\exp\left(-\frac{3}{4}\mathrm{i}\pi\right)\right)\end{pmatrix} = \begin{pmatrix}0\\ \exp\left(-\mathrm{i}\frac{Z^2}{4\delta}\right)\end{pmatrix}, \tag{4.17}$$

which using (4.12) reproduces (4.4) with $S = -1$ (one way to get $S = +1$ would be to replace (4.5) by $\boldsymbol{R} = Y\boldsymbol{e}_Y + Z\boldsymbol{e}_Z$).

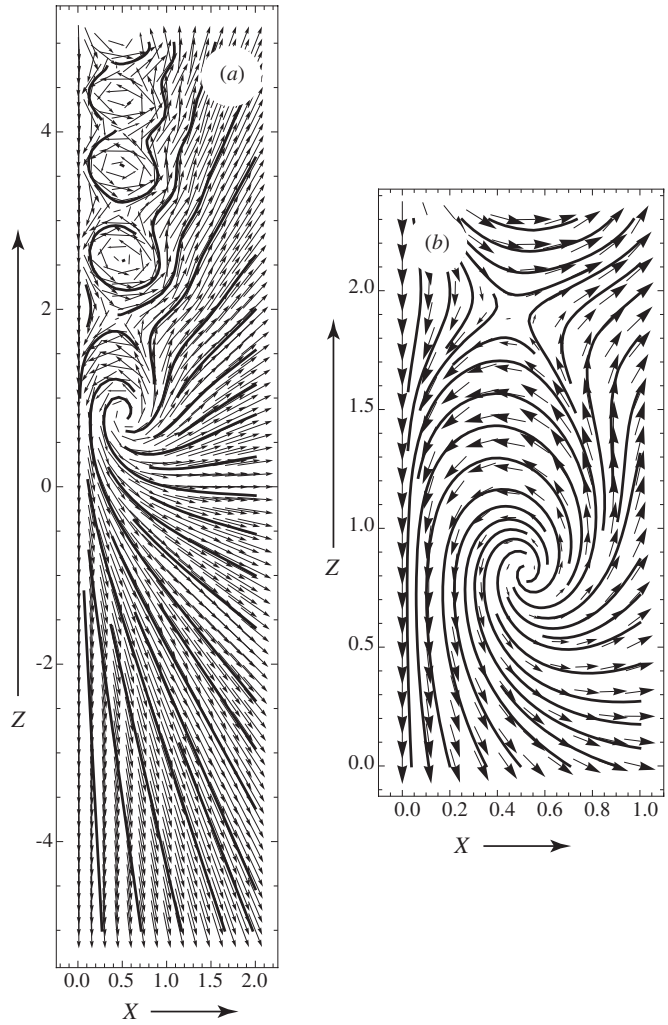

Figure 2. Transverse linearized slow manifold (spin vector field) $\{S_X, S_Z\}$, for $\delta = 0.5$, computed from (4.12) and (4.16), and associated streamlines; (b) is a magnification of (a).

It is easy to compute the spin field (linearized slow manifold) (4.12) corresponding to (4.16). Figure 2 shows the transverse spin field $\{S_X, S_Z\}$ in the XZ plane. On the line $X = 0$, we see that $\boldsymbol{S}(\{0, 0, Z\}, V\boldsymbol{e}_Z) = -\boldsymbol{e}_Z$, as required by the boundary condition. Far from the origin (e.g. along the line $X = 2$ in figure 2(a)), we see $\boldsymbol{S}(\{X, 0, Z\}, V\boldsymbol{e}_Z) \to +\boldsymbol{e}_R$, so the spin points radially, according to the leading-order adiabatic reaction force $\boldsymbol{S}_0$ (equation 4.8).

Also evident from figure 2 are isolated points for small X and positive Z at which the transverse field vanishes. These are singularities of the transverse field, corresponding to the out-of-plane spin S_Y being ± 1. They result from the conflict that occurs for $Z > 0$, between $\boldsymbol{S}$ on the boundary $X = 0$, which points along $-\boldsymbol{e}_Z$, and the adiabatic $\boldsymbol{S}$ far from the origin, where $S_Z > 0$. Since

$$S_Z + \mathrm{i}S_X = |u|^2 - |v|^2 + 2\mathrm{i}\,\mathrm{Re}\,u^*v = (u + \mathrm{i}v)(u^* + \mathrm{i}v^*), \tag{4.18}$$

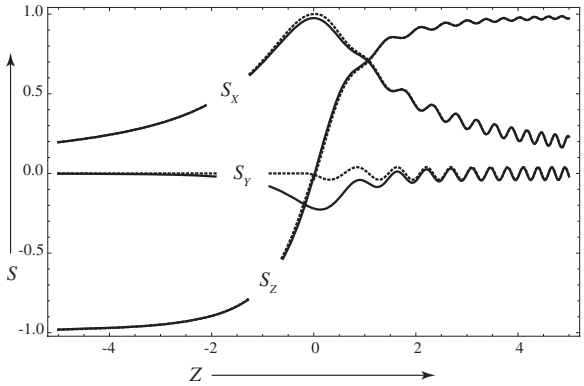

Figure 3. Full curves: components of exact linearized spin field, calculated from (4.12) and (4.16) for $\delta = 0.2$ and $X = 1$. Dotted curves: leading order adiabatic approximation decorated with leading-order exponentially small oscillations, calculated from (4.19).

there are singularities where either factor vanishes. At the singularities, S_X and S_Z vanish linearly, controlled by equations (4.6); but these do not restrict their form. In particular, the transverse field is not divergenceless, so the streamlines can spiral in or out of the singularity, which can therefore be of 'focus' as well as saddle type, as seen in figure 2, where the nonzero divergence is indicated by the fact that the streamlines have ends.

Now we investigate analytically whether the exact linear slow manifold encompasses not only the boundary condition (4.1) at $X = 0$ but also the leading-order adiabatic spin (4.8) for large R (or small δ), which must be decorated with small oscillations that will eventually grow and generate the singularities for small X. This requires asymptotics of the parabolic cylinder functions for large order and large argument simultaneously, namely the Darwin expansions [29]. These are awkward to implement, and it is easier to proceed ab initio as explained in appendix D. To leading orders in the δ-independent and exponentially small terms, the result is

$$\begin{aligned} S_X(X, Z, \delta) &\approx \frac{X}{R} + 2\Theta(Z)\frac{Z}{R}\exp\left(-\frac{\pi X^2}{4\delta}\right)\cos\Gamma \\ S_Y(X, Z, \delta) &\approx -2\Theta(Z)\exp\left(-\frac{\pi X^2}{4\delta}\right)\sin\Gamma \\ S_Z(X, Z, \delta) &\approx \frac{Z}{R} - 2\Theta(Z)\frac{X}{R}\exp\left(-\frac{\pi X^2}{4\delta}\right)\cos\Gamma, \end{aligned} \tag{4.19}$$

where $\Theta(Z)$ denotes the unit step and

$$\Gamma = \frac{1}{\delta}\left(\frac{1}{4}X^2\log\left(\frac{R+Z}{R-Z}\right) + \frac{1}{2}RZ\right). \tag{4.20}$$

This is correctly normalized up to second order in the small exponential. The leading terms in S_X and S_Z give the simplest adiabatic slow manifold $\boldsymbol{S}_0 = \boldsymbol{e}_R$. The corrections give the exponentially small oscillations. Figure 3 shows that this is an excellent approximation. There are slight deviations, especially for S_Y near $Z = 0$, but this is the Stokes line where the small exponential appears discontinuously in this approximation; the discrepancy could be corrected by including more terms of the asymptotic series and smoothing the discontinuity by the universal error function [30–32], but we do not pursue this refinement here.

Equation (4.19) is not the only solution of the Schrödinger lookalike equation (4.15). From any solution $\boldsymbol{S}$, the solution $-\boldsymbol{S}$ is obviously also a solution, because of the linearity of (4.2); it is generated by the transformation

$$\begin{pmatrix} u(X,0,Z,\delta) \\ v(X,0,Z,\delta) \end{pmatrix} \quad \Rightarrow \quad \begin{pmatrix} v^*(X,0,Z,\delta) \\ -u^*(X,0,Z,\delta) \end{pmatrix}, \tag{4.21}$$

which also satisfies (4.15). The alternative transformation

$$\begin{pmatrix} u(X,0,Z,\delta) \\ v(X,0,Z,\delta) \end{pmatrix} \quad \Rightarrow \quad \begin{pmatrix} v^*(X,0,-Z,\delta) \\ u^*(X,0,-Z,\delta) \end{pmatrix}, \tag{4.22}$$

also satisfies (4.15) and generates the following spin field, symmetry-related to that illustrated in figure 2:

$$\boldsymbol{S}(X,0,Z,\delta) \Rightarrow \{S_X(X,0,-Z,\delta), S_Y(X,0,-Z,\delta), -S_z(X,0,-Z,\delta)\}. \tag{4.23}$$

In the linearization discussed in this section, no use has been made of the solutions (3.5) of the exact equations, involving the constant J, because these are not solutions of the approximate equations (4.1).

5. Numerical illustrations of precession suppression

We expect that the spin precession, and the oscillations that it causes in the force on the slow particle, will be increasingly suppressed as more adiabatic reaction forces are included in the slow manifold series. To study this, we compute numerical solutions of the slow dynamics equation (2.6), with the constant of motion $\boldsymbol{J}$ fixed by initial conditions corresponding to the Nth-order slow manifold for the initial slow variables $\boldsymbol{R}_0$, $\boldsymbol{V}_0$. We define

$$\boldsymbol{S}_{\mathrm{slow},N}(\boldsymbol{R},\boldsymbol{V}) \equiv \frac{\sum_{n=0}^{N} \varepsilon^n \boldsymbol{S}_n(\boldsymbol{R},\boldsymbol{V})}{\left|\sum_{n=0}^{N} \varepsilon^n \boldsymbol{S}_n(\boldsymbol{R},\boldsymbol{V})\right|}. \tag{5.1}$$

(Without the denominator to enforce normalization, we would have $|\boldsymbol{S}_{\mathrm{slow},N}| = 1 + \mathrm{O}(\varepsilon^{N+1})$.) Then the constant of motion is

$$\boldsymbol{J}_N(\boldsymbol{R}_0,\boldsymbol{V}_0) = \boldsymbol{R}_0 \times \boldsymbol{V}_0 + \boldsymbol{S}_{\mathrm{slow},N}(\boldsymbol{R}_0,\boldsymbol{V}_0). \tag{5.2}$$

We denote the corresponding slow trajectories – exact solutions of (2.6) – by

$$\boldsymbol{R}_N(t;\boldsymbol{R}_0,\boldsymbol{V}_0), \boldsymbol{V}_N(t;\boldsymbol{R}_0,\boldsymbol{V}_0). \tag{5.3}$$

To gauge the effectiveness of the slow manifold, we compare two reaction forces. The first is the force along the exact trajectory at time t:

$$\boldsymbol{F}_N(t;\boldsymbol{R}_0,\boldsymbol{V}_0) = \dot{\boldsymbol{V}}_N(t;\boldsymbol{R}_0,\boldsymbol{V}_0). \tag{5.4}$$

The second is the force corresponding to the slow manifold at the particle's position and velocity at time t:

$$\boldsymbol{F}_{\mathrm{slow},N}(t;\boldsymbol{R}_0,\boldsymbol{V}_0) = -\boldsymbol{S}_{\mathrm{slow},N}(\boldsymbol{R}_N(t;\boldsymbol{R}_0,\boldsymbol{V}_0),\boldsymbol{V}_N(t;\boldsymbol{R}_0,\boldsymbol{V}_0)). \tag{5.5}$$

The difference between $\boldsymbol{F}_N$ and $\boldsymbol{F}_{\mathrm{slow},N}$ is a measure of how closely the particle clings to the Nth order slow manifold. Exploiting rotational symmetry, we can without loss of generality choose

$$\boldsymbol{R}_0 = \{0,0,R_0\}, \qquad \boldsymbol{V}_0 = \{V_{\perp 0},0,V_{\parallel 0}\}. \tag{5.6}$$

For each choice of $R_0, V_{\perp 0}, V_{\parallel 0}$ and the order N, there are two cases, corresponding to $S = \pm 1$.

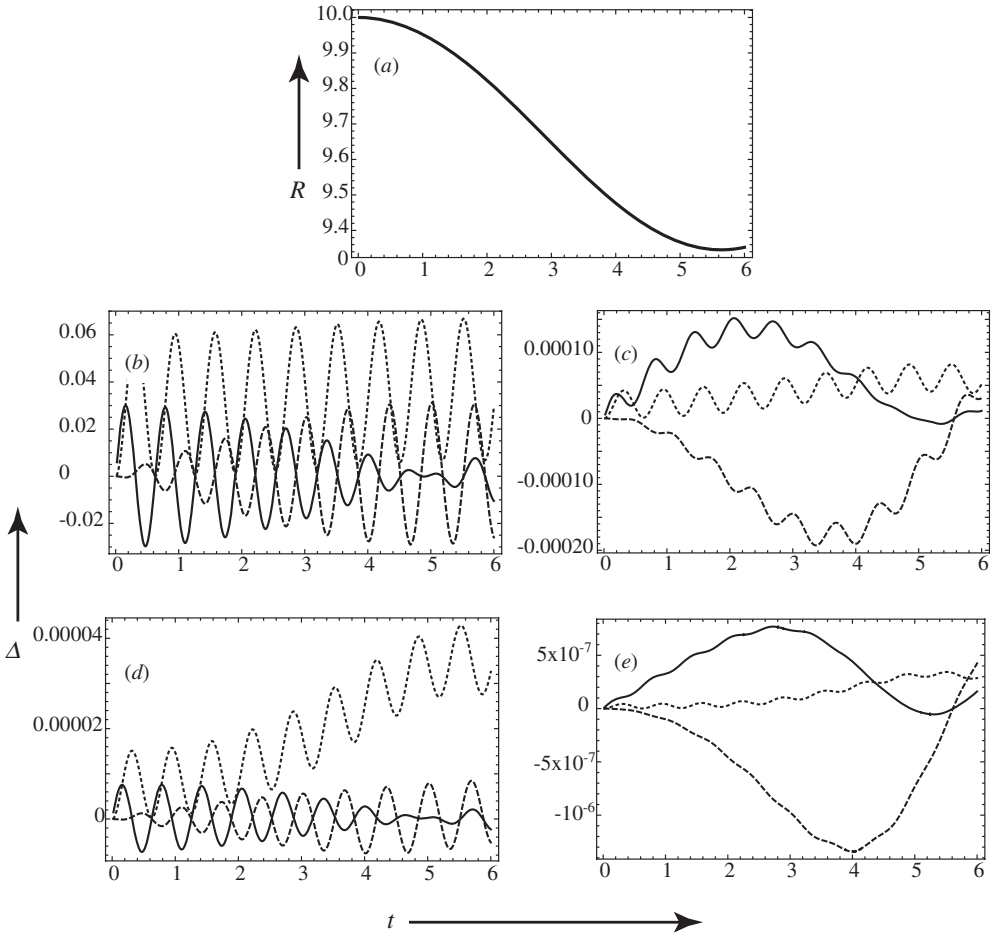

Figure 4. (*a*) Distance from the origin for $\varepsilon = 1$ and the attractive case $S = +1$ and initial conditions $R_0 = 10$, $V_{\perp 0} = 3$, $V_{\parallel 0} = 0$. (*b–e*): difference vectors Δ_N (equation (5.7)) between the exact force and the force on the Nth order slow manifold for (*b*) $N = 0$, (*c*) $N = 1$, (*d*) $N = 2$, (*e*) $N = 3$ (full curves: x components; dotted curves,y components; dashed curves: z components). Note the very different vertical scales, indicating closer following of the slow manifold as N increases. Computations were carried out using Runge–Kutta integration of the differential equations (2.6).

Figures 4 and 5 show the differences

$$\boldsymbol{\Delta}_N \equiv \boldsymbol{F}_N - \boldsymbol{F}_{\text{slow},N} \tag{5.7}$$

along two different trajectories, with $S = +1$ (attractive lowest-order dynamics) and $S = -1$ (repulsive lowest-order dynamics). In both cases, the accuracy with which the trajectories follow the slow manifold improves dramatically as N increases. The improvement with N is faster for the atttactive case (figure 4) than for repulsion (figure 5), probably because $R(t)$ varies more slowly in the attractive case: between 10.0 and 9.4 between $t = 0$ and $t = 6$ compared with between 10 and 20 between $t = 0$ and $t = 3$ for repulsion.

The connection between oscillations and the Stokes phenomenon when $\boldsymbol{R} \cdot \boldsymbol{V} = 0$, demonstrated for the linearized slow manifold, strongly suggests that as soon as the distance

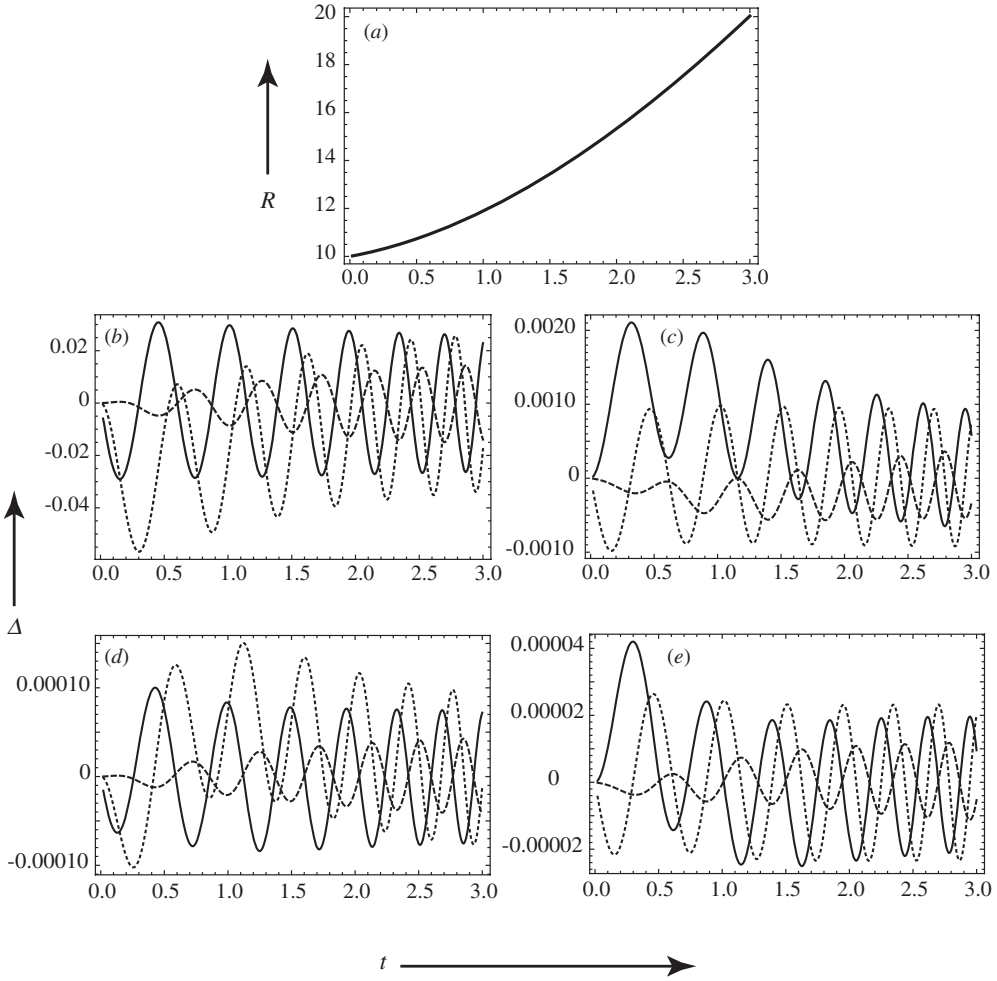

Figure 5. As figure 4, for the repulsive case $S = -1$ and initial conditions $R_0 = 10$, $V_{\perp 0} = 3$, $V_{\parallel 0} = 1$.

of a trajectory from the origin is a minimum, the spin along the trajectory will begin to exhibit oscillatory deviations from that on the Nth order slow manifold, because this does not incorporate the exponentially small fast oscillations that are expected to decorate the exact slow manifold. Figure 6 indicates that this happens. The particle falls towards the origin until $t = t_c \sim 3.2$, and then recedes (figure 6(a)). For $t < t_c$ increasing N makes the spin cling closer to the slow manifold. After t_c, the oscillatory deviation from the slow manifold is nearly the same for $N = 2$ and $N = 3$, and moreover does not diminish as R increases (when the naive asymptotics should improve).

6. High-order reaction forces

Because the recurrence relations (3.10) for the slow manifold coefficients $\boldsymbol{S}_n(\boldsymbol{R}, \boldsymbol{V})$ involve derivatives with respect to $\boldsymbol{R}$ and $\boldsymbol{V}$, it is to be expected on the basis of Darboux's principle

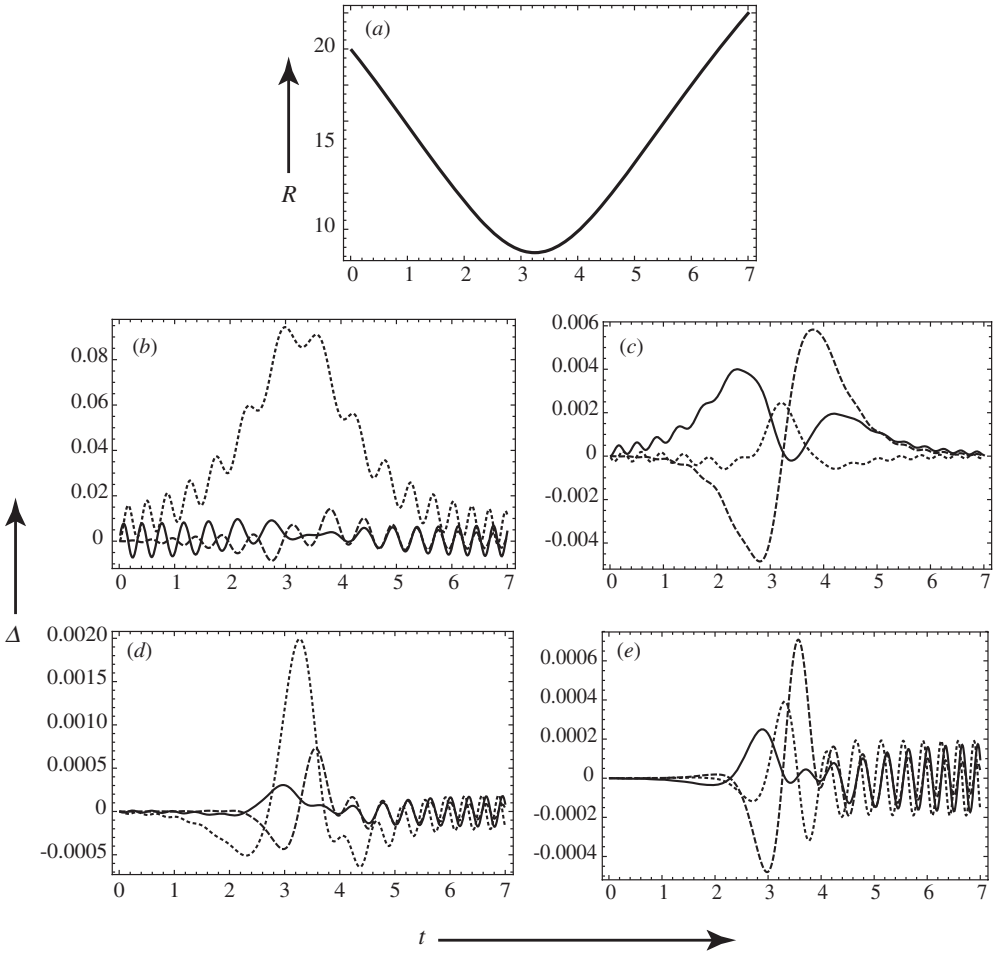

Figure 6. As figure 4, for $\varepsilon = 1$ and the attractive case $S = +1$ and initial conditions $R_0 = 20$, $V_{\perp 0} = 3$, $V_{\parallel 0} = -4$, indicating the appearance and persistence of oscillations after the particle passes closest to the origin.

[33] that the series will diverge factorially. If the signs of the components of $\boldsymbol{S}_n$ in the terms alternate as n increases (either successively or in a pattern where several positive terms are followed by several negative ones), the series is Borel-summable and the divergent tail of the series when truncated at the term $\boldsymbol{S}_n$ can be well approximated by a multiple of $\boldsymbol{S}_{n+1}$, giving an exponentially small termination when n corresponds to the least term of the asymptotic series (optimal truncation). This procedure fails if the signs are all the same, which occurs on a hypersurface in the slow phase space $\{\boldsymbol{R}, \boldsymbol{V}\}$. Across this 'Stokes surface', an exponentially small contribution appears [33, 34].

In the present problem, it is known from studies of the slaved spin dynamics (equation (2.4) with prescribed $\boldsymbol{R}(t)$) that the Stokes phenomenon is associated with minima of $R(t)$, that is $\boldsymbol{R}$ and $\boldsymbol{V}$ orthogonal. In the coupled problem (hamiltonian (2.1)), we have already seen this in the linearized slow manifold (section 4): from the exact solution of the Landau–Majorana–Zener model [22–24], the exponentially small contributions, with associated fast oscillations (equations (4.19)), appear when $X = 0$, which indeed corresponds to $\boldsymbol{R} \cdot \boldsymbol{V} = 0$.

But for the nonlinear slow manifold, there is a subtlety, associated with the fact that $\boldsymbol{R}\cdot\boldsymbol{V}=0$ can correspond not only to a minimum of $R(t)$ but also to a maximum, for which we do not expect a Stokes phenomenon. Physically it is clear why this is so: the adiabatic approximation fails when R is closest to the origin, not when it is farthest. Mathematically, oscillations appear when a Stokes line from a complex zero t_c, satisfying $R(t_c)=0$, crosses the real axis of the complex-time plane; and as elementary examples indicate, such complex zeros are associated with minima of $R(t)$ but not maxima. Incorporating this insight, in order to anticipate the behaviour of the signs of the high-order slow manifold cofficients, requires knowledge of the gross features of the slow dynamics, as given by the Born–Oppenheimer approximation, which we elucidate now.

From (3.2), the conserved energy in this lowest-order approximation is

$$E=\varepsilon\frac{P^2}{2}+\frac{SR}{\varepsilon}=\frac{1}{\varepsilon}\left(\frac{1}{2}V^2+SR\right). \tag{6.1}$$

Also conserved is the angular momentum, involving the velocity component perpendicular to $\boldsymbol{R}$:

$$L=RV_\perp=R\sqrt{V^2-V_\parallel^2}. \tag{6.2}$$

We are interested in the case $\boldsymbol{R}\cdot\boldsymbol{V}=0$, that is $V_\parallel=0$. For repulsive Born–Oppenheimer dynamics, where $S<0$, $V_\parallel=0$ always corresponds to minima of $R(t)$ along trajectories, so we expect a Stokes phenomenon (all terms with the same sign) whenever $\boldsymbol{R}\cdot\boldsymbol{V}=0$. For attractive Born–Oppenheimer dynamics, where $S>0$, $\boldsymbol{R}\cdot\boldsymbol{V}=0$ can correspond either to a maximum R_+, where the speed is V_+, or a minimum R_-, where the speed is V_-. To distinguish these cases, we note that combining (6.1) and (6.2) for $V_\parallel=0$ gives

$$\frac{L^2}{2R_+^2}+SR_+=\frac{L^2}{2R_-^2}+SR_-. \tag{6.3}$$

The minimum of this effective radial potential is given by $R^3=L^2/S$, i.e. $V^2/R=S$. Thus maxima R_+ correspond to $V^2/R<S$, and in this case we do not anticipate a Stokes phenomenon. Minima of R_- correspond to $V^2/R>S$, and we do anticipate a Stokes phenomenon.

To calculate the high-order spin field coefficients $\boldsymbol{S}_n$, it is convenient to express them in component form, in the basis defined by the following unit vectors:

$$\boldsymbol{e}_R\equiv\frac{\boldsymbol{R}}{R},\qquad \boldsymbol{e}_2\equiv\frac{\boldsymbol{e}_R\times\boldsymbol{V}}{|\boldsymbol{e}_R\times\boldsymbol{V}|}=\frac{\boldsymbol{e}_R\times\boldsymbol{e}_V}{\sqrt{1-(\boldsymbol{e}_R\cdot\boldsymbol{e}_V)^2}},\qquad \boldsymbol{e}_3\equiv\boldsymbol{e}_R\times\boldsymbol{e}_2. \tag{6.4}$$

It follows from the determining equations (3.10) and (3.12) that the odd spin coefficients depend only on $\boldsymbol{e}_R$ and $\boldsymbol{e}_3$, and the even coefficients depend only on $\boldsymbol{e}_2$. In a further simplification, motivated by (2.8), we define the R-scaled speed by

$$U\equiv\frac{V}{\sqrt{R}}, \tag{6.5}$$

from which it can be shown that $\boldsymbol{S}_n\propto R^{-3n/2}$. With R thus eliminated, the coefficients depend only on two variables: U, and

$$T\equiv\boldsymbol{e}_R\cdot\boldsymbol{e}_V=\cos\theta. \tag{6.6}$$

where θ is the angle between $\boldsymbol{R}$ and $\boldsymbol{V}$. In terms of the variables U and T, the Stokes phenomenon, anticipated on the basis of the analysis of the Born–Oppenheimer dynamics, is expected to occur when $T=0$, for all values of U when $S=-1$, and for $U>1$ when $S=+1$.

Thus we represent the coefficients in the following convenient form:

$$\begin{aligned}\boldsymbol{S}_{2n}(\boldsymbol{R},\boldsymbol{V}) &= \frac{1}{R^{3n}}(\alpha_n(U,T)\boldsymbol{e}_R + U\sqrt{1-T^2}\gamma_n(U,T)\boldsymbol{e}_3),\\ \boldsymbol{S}_{2n+1}(\boldsymbol{R},\boldsymbol{V}) &= \frac{U\sqrt{1-T^2}}{R^{3n+3/2}}\beta_n\,(U,T)\,\boldsymbol{e}_2.\end{aligned} \tag{6.7}$$

Derivation of the recurrence relations satisfied by the functions $\alpha_n(U,T)$, $\beta_n(U,T)$ and $\gamma_n(U,T)$ is facilitated by the following formulas, which hold for any unit vector $\boldsymbol{e}$:

$$\begin{aligned}&\boldsymbol{U}\cdot\nabla_{\boldsymbol{R}}\boldsymbol{e} = \frac{U\sqrt{1-T^2}}{R}\boldsymbol{e}_2\times\boldsymbol{e},\\ &\boldsymbol{e}_R\cdot\nabla_U\boldsymbol{e} = \boldsymbol{e}_3\cdot\nabla_U\boldsymbol{e} = 0, \qquad \boldsymbol{e}_2\cdot\nabla_U\boldsymbol{e} = \frac{1}{U\sqrt{1-T^2}}\boldsymbol{e}_R\times\boldsymbol{e}.\end{aligned} \tag{6.8}$$

The relations are

$$\begin{aligned}\beta_n = {}&-\alpha_n - 3UT\left(n+\frac{1}{2}\right)\gamma_n - \frac{1}{2}U^2T\partial_U\gamma_n + U(1-T^2)\partial_T\gamma_n\\ &-\sum_{m=0}^{n-1}\beta_{n-m-1}\beta_m - \sum_{m=1}^{n}\left(\alpha_{n-m}\left(T\partial_U\gamma_m + \frac{1-T^2}{U}\partial_T\gamma_m\right)\right.\\ &\left.-U(1-T^2)\gamma_{n-m}\left(\partial_U\gamma_m - \frac{T}{U}\partial_T\gamma_m\right) - \gamma_{n-m}\gamma_m\right),\\ \gamma_n = {}&3nUT\beta_{n-1} + \frac{1}{2}U^2T\partial_U\beta_{n-1} - U(1-T^2)\partial_T\beta_{n-1}\\ &+\sum_{m=0}^{n-1}\left(\alpha_{n-m-1}\left(T\partial_U\beta_m + \frac{1-T^2}{U}\partial_T\beta_m\right)\right.\\ &\left.-U(1-T^2)\gamma_{n-m-1}\left(\partial_U\beta_m - \frac{T}{U}\partial_T\beta_m\right) - 2\beta_{n-m-1}\gamma_m\right),\\ \alpha_n = {}&-\frac{1}{2S}\left[\sum_{m=1}^{n-1}(\alpha_{n-m}\alpha_m + U^2(1-T^2)(\gamma_{n-m}\gamma_m + \beta_{n-m-1}\beta_m)) - SU^2(1-T^2)\beta_{n-1}\right],\end{aligned} \tag{6.9}$$

with the initial conditions

$$\alpha_0 = S, \qquad \gamma_0 = 0. \tag{6.10}$$

Thus the coefficients enabling the calculation of $\boldsymbol{S}_0$ through $\boldsymbol{S}_7$ are calculated to be

$$\alpha_0 = S, \qquad \beta_0 = -S, \qquad \gamma_0 = 0$$

$$\alpha_1 = \frac{1}{2}SU^2(T^2-1), \qquad \beta_1 = \frac{1}{2}S(4S+5U^2(7T^2-1)), \qquad \gamma_1 = -3SUT$$

$$\alpha_2 = -\frac{1}{8}SU^2(T^2-1)(16S+21U^2(5T^2-1))$$

$$\beta_2 = -\frac{1}{8}S(256S^2+32SU^2(161T^2-20)+21U^4(715T^4-374T^2+19))$$

$$\gamma_2 = \frac{3}{2}SUT(24S+35U^2(3T^2-1))$$

$$\alpha_3 = \frac{1}{16}SU^2(T^2-1)(544S^2+32SU^2(286T^2-43)+11U^4(2275T^4-1274T^2+79))$$

$$\beta_3 = \frac{1}{16}S(20\,224S^3 + 864S^2U^2(841T^2 - 89) + 96SU^4(47\,740T^4 - 22\,293T^2 + 998)$$
$$+715U^6(11\,305T^6 - 10\,353T^4 + 2127T^2 - 55))$$
$$\gamma_3 = -\frac{3}{8}SUT(3552S^2 + 16SU^2(2137T^2 - 617) + 231U^4(325T^4 - 234T^2 + 29)) \qquad (6.11)$$

The coefficients have the following structure:

$$\alpha_n = S\sum_{l=1}^{n} U^{2l}S^{n-l}\sum_{j=0}^{l} a_{n,j,l}T^{2j},$$
$$\beta_n = S\sum_{l=0}^{n} U^{2l}S^{n-l}\sum_{j=0}^{l} b_{n,j,l}T^{2j}, \qquad (6.12)$$
$$\gamma_n = SUT\sum_{l=0}^{n-1} U^{2l}S^{n-l-1}\sum_{j=0}^{l} c_{n,j,l}T^{2j}.$$

We do not give here the recurrence relations for $a_{n,j,l}$, $b_{n,j,l}$, and $c_{n,j,l}$, derived from (6.9); they are nonlinear, reflecting the nonlinearity of the slow manifold equation (3.4). A general analytic solution seems difficult.

However, as expected from the linearization of section 4 the equations for the coefficients of the highest powers of U are linear and can be solved explicitly, starting from the highest powers of T. These coefficients are

$$a_{n,n-k,n} = \text{coefficient of } SU^{2n}T^{2(n-k)} \quad \text{in } \alpha_n,$$
$$b_{n,n-k,n} = \text{coefficient of } SU^{2n}T^{2(n-k)} \quad \text{in } \beta_n, \qquad (6.13)$$
$$c_{n+1,n-k,n} = \text{coefficient of } SU^{2n+1}T^{2(n-k)+1} \quad \text{in } \gamma_{n+1}, \quad (0 \leqslant k \leqslant n)$$

For the first few k, these coefficients (equivalent to the Darwin expansions of parabolic cylinder functions [29]) are

$$a_{n,n,n} = -\left(-\frac{1}{3}\right)^n 2^{2n-1}\frac{\Gamma\left(3n-\frac{1}{2}\right)}{\sqrt{\pi}\Gamma(n+1)},$$
$$b_{n,n,n} = -\left(-\frac{1}{3}\right)^n 2^{2n+1}\frac{\Gamma\left(3n+\frac{3}{2}\right)}{\sqrt{\pi}\Gamma(n+1)},$$
$$c_{n+1,n,n} = -\left(-\frac{1}{3}\right)^n 4^{n+1}\frac{\Gamma\left(3n+\frac{5}{2}\right)}{\sqrt{\pi}\Gamma(n+1)},$$
$$a_{n,n-1,n} = -\left(-\frac{4}{3}\right)^{n-1}(4n+1)\frac{\Gamma\left(3n-\frac{3}{2}\right)}{5\sqrt{\pi}\Gamma(n)},$$
$$b_{n,n-1,n} = \left(-\frac{4}{3}\right)^n(12n-7)\frac{\Gamma\left(3n+\frac{1}{2}\right)}{5\sqrt{\pi}\Gamma(n)},$$
$$c_{n+1,n-1,n} = \left(-\frac{4}{3}\right)^n(4n+1)\frac{6\Gamma\left(3n+\frac{3}{2}\right)}{5\sqrt{\pi}\Gamma(n)},$$
$$a_{n,n-2,n} = -\left(-\frac{4}{3}\right)^n\left(336n^2-160n-289\right)\frac{3\Gamma\left(3n-\frac{5}{2}\right)}{2800\sqrt{\pi}\Gamma(n-1)},$$

$$b_{n,n-2,n} = \left(-\frac{4}{3}\right)^n \left(1008n^2 - 2016n + 953\right) \frac{\Gamma\left(3n - \frac{1}{2}\right)}{720\sqrt{\pi}\,\Gamma\,(n-1)},$$
$$c_{n+1,n-2,n} = -\left(-\frac{4}{3}\right)^n \left(336n^2 - 160n - 9\right) \frac{3\Gamma\left(3n + \frac{1}{2}\right)}{350\sqrt{\pi}\,\Gamma\,(n-1)}. \tag{6.14}$$

As k increases, the calculations get more intricate, and we have not seen a pattern.

We are interested in the large n behaviour. For these coefficients of U^{2n}, Stirling's formula (or the asymptotics of the recurrence relations) gives

$$\left.\begin{aligned} a_{n,n-k,n} &\to (-1)^{n+k+1} \frac{9^n \Gamma\,(2n+k-1)}{5^{k+1} 3\pi k!} \\ b_{n,n-k,n} &\to (-1)^{n+k+1} \frac{9^n 3\Gamma\,(2n+k+1)}{5^{k+1} \pi k!} \\ c_{n+1,n-k,n} &\to (-1)^{n+k+1} \frac{9^{n+1} \Gamma\,(2n+k+2)}{5^{k+1} \pi k!} \end{aligned}\right\} \quad (n \to \infty, k \text{ fixed}) \tag{6.15}$$

We see the expected factorial divergence. The coefficients diverge factorially, so, for these large values of U and high powers of T,

$$|\boldsymbol{S}_n| \sim \frac{U^n}{R^{3n/2}} n! = \left(\frac{V}{R^2}\right)^n n!. \tag{6.16}$$

The signs in the coefficients (6.15) alternate with k as well as n, so if many terms l, j contribute in the series (6.12) it is not easy to identify the pattern of signs in the sequence of $\boldsymbol{S}_n$. The small-k coefficients in (6.15) correspond to the high powers of T as well as U, and if $|T| \gg 1$ they would dominate, indicating an alternating-sign series and the expected absence of the Stokes phenomenon. But T can never exceed unity (cf (6.6)), so the implication of the signs in (6.15) is obscure.

In fact, the most interesting case is $T = 0$, i.e. $\boldsymbol{V}$ perpendicular to $\boldsymbol{R}$, corresponding for the slaved-spin case and the linearization to the Stokes line, across which an exponentially small precessing spin component develops. But when $T = 0$ the contributing coefficients are $k = n$ in (6.13) (cf (6.12)), and this case is excluded in the asymptotics (6.15). Nevertheless, these coefficients can be computed from (6.9). It suffices to consider just the coefficients $b_{n,0,n}$ (the a and c coefficients are similar); they are very accurately fitted by

$$b_{n,0,n} = C \left(\frac{4}{\pi}\right)^{2n} \Gamma(2n+1), \tag{6.17}$$

where C is a constant. Here all the terms have the same sign, so we do expect a Stokes phenomenon. Standard asymptotics for the summation of the divergent tail of the series of $\boldsymbol{S}_n$ in (6.7) and (6.12), leads to the associated small exponential $\exp(-4R^2/\pi\varepsilon V)$, precisely concordant with that in (4.19) on recalling that $\delta = \varepsilon V$.

The formulas (6.13)–(6.19) correspond to the highest powers of U contributing to each of the $\boldsymbol{S}_n$, and so represent only the linearized slow manifold. However, by computer-algebra solution of (6.9) it is possible to calculate the coefficients exactly, and identify the signs, for any values of U, T and $S = \pm 1$, up to large values of n.

Our investigations for $n < 50$ show the following. The magnitudes $|\boldsymbol{S}_n|$ always increase factorially. The pattern of signs depends on U, T and S. When $T \neq 0$ it is alternating. Sometimes the alternation is erratic (at least for $n < 50$) and sometimes it is regular; for example, when $U = 3/2$, $T = 1/2$, $S = 1$, the signs of β_n are --++--++--.... Alternating signs indicate a series that is Borel-summable, and terminating the sum over $\boldsymbol{S}_n$ at the least term, which from

(6.16) corresponds to $n \sim R^2/\varepsilon V$, leaves a remainder given by the first omitted term, times a constant that depends on the pattern of signs.

When $T = 0$, we find that for $S = -1$ all coefficents n have the same sign for all U, and for $S = +1$ the coefficients have the same sign when $U > 1$ but alternate when $U < 1$, exactly as anticipated at the beginning of this section from analyzing the Born–Oppenheimer dynamics. Another approach leading to the same conclusion is analysis of the real zeros $w_{n,m}$ of the real polynomials

$$P_n(w, T) = \sum_{l=0}^{n} w^l \sum_{j=0}^{l} b_{n,j,l} T^{2j} \tag{6.18}$$

for different values of T and (large) n. These polynomials determine the coefficients β_n according to (6.12), for $S = \pm 1$, because

$$\beta_n = S^{n+1} P_n(SU^2, T). \tag{6.19}$$

The $w_{n,m}$ depend on n, so if U is in a region where there are zeros the signs of P_n, and hence of β_n, will alternate. We find that for $T \neq 0$ the $w_{n,m}$ spread along the whole real axis as n increases. But when $T = 0$ the $w_{n,m}$ all lie in the interval $0 < w < 1$ (there are also complex zeros, clustering closer to $w = 1$ as n increases). Since $w = SU^2$, the range of U does not include these zeros if $S = -1$, so the coefficient signs do not alternate. But for $S = +1$ only the interval $1 < U < \infty$ is free of zeros; if $0 < U < 1$ there are zeros, and the signs alternate.

7. Concluding remarks

The model (2.1) that we have explored here, of a particle whose spin is coupled to its position, is a simple yet nontrivial system for which the high-order reaction forces, whose sum would determine the slow manifold, is studied in detail. It is a simplification of the model of appendix A which, although itself a simplification of the general case of hamiltonian fast-slow coupling, generates high-order reactions that soon get intractably complicated. For the spin model, we calculated high-order reaction forces, in an attempt to find a slow manifold to which the spin would cling forever, without oscillating.

The series of reaction forces diverges. The divergence is particularly severe when all terms have the same sign. This happens where the slow vectors $\boldsymbol{R}$ and $\boldsymbol{V}$ are orthogonal and $V^2/R > S$, corresponding to a minimum of the distance $R(t)$. It represents a Stokes phenomenon, signalling the appearance of weak fast oscillations in the slow variable, and precession in the spin—as in the slaved-spin case. General studies [35, 36] have proved the persistence of nonoscillatory solutions, clinging close to a slow manifold, only up to a finite time. Consistent with this, our numerical solutions of the trajectory equations show the spin clinging closer to the higher-order slow manifolds (figures 4 and 5), but eventually oscillating around it, with the oscillations beginning when $R(t)$ is stationary (figure 6). Oscillations seem unavoidable. (There exist families of nonoscillatory driving histories $\boldsymbol{R}(t)$ for which the spin does not precess [37], but these do not seem relevant to the slow manifold associated with (2.1).)

Interpreting the divergence in terms of the Stokes phenomenon would lead to an exact solution for the slow manifold in the particle phase space, to which the spin would cling forever. But because this manifold would contain exponentially weak fast oscillations in the particle's phase space, it is, as pointed out in the Introduction, something of a misnomer to call it 'slow'.

We have not been able to find, and cannot prove the existence of, exact solutions of the nonlinear slow manifold equation (3.4) with the asymptotic condition (3.2) and the boundary

condition (3.6). The only approaches we could implement are the divergent ε-series and the exact solutions of the linearized slow manifold equation (4.1), both of which support the statements in the preceding paragraphs.

Acknowledgments

We thank Professor Robert Mackay for introducing us to slow-manifold theory, especially his review [4], and for helpful comments on the paper, for which we also thank Professor John Hannay and Dr Jonathan Robbins. MVB's research is supported by the Leverhulme Trust.

Appendix A. First-order reaction force (geometric magnetism) in a generalized model

In this generalization of (2.1), the fast system has (possibly multidimensional) phase-space variables $\boldsymbol{x} = \{\boldsymbol{q}, \boldsymbol{p}\}$, and is incorporated into the hamiltonian by a potential Φ, according to

$$H = \frac{1}{2}\varepsilon \boldsymbol{P}\cdot\boldsymbol{P} + \frac{1}{\varepsilon}\Phi\left(\boldsymbol{R}, \boldsymbol{x}\right). \tag{A.1}$$

The slow velocity is

$$\boldsymbol{V} \equiv \dot{\boldsymbol{R}} = \varepsilon \boldsymbol{P}, \tag{A.2}$$

and the corresponding force is

$$\boldsymbol{\mathcal{F}}\left(\boldsymbol{R}, \boldsymbol{x}\right) \equiv \ddot{\boldsymbol{R}} = \dot{\boldsymbol{V}} = \varepsilon\dot{\boldsymbol{P}} = -\nabla_{\boldsymbol{R}}\Phi(\boldsymbol{R}, \boldsymbol{x}). \tag{A.3}$$

The fast dynamics is

$$\dot{\boldsymbol{x}} = \frac{1}{\varepsilon}\mathbf{J}\nabla_x\Phi(\boldsymbol{R}, x) \equiv \frac{1}{\varepsilon}\boldsymbol{v}(\boldsymbol{R}, \boldsymbol{x}), \tag{A.4}$$

involving the symplectic matrix, with elements corresponding to $\boldsymbol{q}$ and $\boldsymbol{p}$,

$$\mathbf{J} = \begin{Bmatrix} 0 & 1 \\ -1 & 0 \end{Bmatrix}. \tag{A.5}$$

Assume now that if the slow variables are regarded as fixed, the fast dynamics possesses an equilibrium state, in which $\boldsymbol{r}$ and $\boldsymbol{p}$ do not change. This determines an approximation to the slow manifold:

$$\boldsymbol{v}(\boldsymbol{R}, \boldsymbol{x}_0) = 0 \Rightarrow \boldsymbol{x} = \boldsymbol{x}_0(\boldsymbol{R}), \tag{A.6}$$

and the corresponding 'Born–Oppenheimer' force on the slow dynamics:

$$\boldsymbol{F}_0(\boldsymbol{R}) = \boldsymbol{\mathcal{F}}(\boldsymbol{R}, \boldsymbol{x}_0(\boldsymbol{R})). \tag{A.7}$$

If a corresponding exact slow manifold exists when the slow velocity $\boldsymbol{V} \neq 0$, it must be a function on the slow phase space, denoted

$$\boldsymbol{x} = \boldsymbol{x}_{\mathrm{c}}(\boldsymbol{R}, \boldsymbol{V}). \tag{A.8}$$

The equation that $\boldsymbol{x}_{\mathrm{c}}$ must satisfy is determined by the fast velocity on it:

$$\dot{\boldsymbol{x}}_{\mathrm{c}} = \dot{\boldsymbol{R}}\cdot\nabla_{\boldsymbol{R}}\boldsymbol{x}_{\mathrm{c}} + \dot{\boldsymbol{V}}\cdot\nabla_{\boldsymbol{V}}\boldsymbol{x}_{\mathrm{c}} = \boldsymbol{V}\cdot\nabla_{\boldsymbol{R}}\boldsymbol{x}_{\mathrm{c}} + \boldsymbol{\mathcal{F}}(\boldsymbol{R}, \boldsymbol{x}_{\mathrm{c}})\cdot\nabla_{\boldsymbol{V}}\boldsymbol{x}_{\mathrm{c}}. \tag{A.9}$$

After incorporating the fast dynamics (A.4), we get the slow manifold equation

$$\frac{1}{\varepsilon}\boldsymbol{v}\left(\boldsymbol{R}, \boldsymbol{x}_{\mathrm{c}}\right) = \boldsymbol{V}\cdot\nabla_{\boldsymbol{R}}\boldsymbol{x}_{\mathrm{c}} + \boldsymbol{\mathcal{F}}(\boldsymbol{R}, \boldsymbol{x}_{\mathrm{c}})\cdot\nabla_{\boldsymbol{V}}\boldsymbol{x}_{\mathrm{c}}. \tag{A.10}$$

This is the generalization of (3.4) determining the slow manifold in the spin model. The solution, if it exists, determines the force on the slow particle according to

$$\boldsymbol{F}(\boldsymbol{R}, \boldsymbol{V}) = \boldsymbol{\mathcal{F}}(\boldsymbol{R}, \boldsymbol{x}_{\mathrm{c}}(\boldsymbol{R}, \boldsymbol{V})). \tag{A.11}$$

We seek the slow manifold as an adiabatic series:

$$\boldsymbol{x}_{\mathrm{c}}(\boldsymbol{R},\boldsymbol{V}) = \boldsymbol{x}_0(\boldsymbol{R}) + \sum_{n=1}^{\infty} \varepsilon^n \boldsymbol{x}_n(\boldsymbol{R},\boldsymbol{V}). \tag{A.12}$$

To find the first correction, we substitute into (A.10), extract the terms independent of ε, and note that $\boldsymbol{x}_0$ is independent of $\boldsymbol{V}$, leading to

$$\boldsymbol{x}_1(\boldsymbol{R},\boldsymbol{V}) \cdot \nabla_{\boldsymbol{x}} \boldsymbol{v}\,(\boldsymbol{R},\boldsymbol{x}_0) = \boldsymbol{V} \cdot \nabla_{\boldsymbol{R}} \boldsymbol{x}_0(\boldsymbol{R}). \tag{A.13}$$

Writing this in component form

$$M_{ij} x_{1j} = b_i, \tag{A.14}$$

where the indices i, j label fast phase-space variables and

$$b_i = (\boldsymbol{b})_i = \boldsymbol{V} \cdot \nabla_{\boldsymbol{R}} \boldsymbol{x}_{0i}(\boldsymbol{R}), \qquad M_{ij} = (\mathbf{M})_{ij} = \partial_{x_j} v_i, \tag{A.15}$$

gives the solution

$$\boldsymbol{x}_1 = \mathbf{M}^{-1}\boldsymbol{b}. \tag{A.16}$$

The corresponding first-order reaction force, correcting (A.7), is

$$\boldsymbol{F}_1(\boldsymbol{R},\boldsymbol{V}) = \boldsymbol{x}_1(\boldsymbol{R},\boldsymbol{V}) \cdot \nabla_{\boldsymbol{x}} \boldsymbol{\mathcal{F}}(\boldsymbol{R}, \boldsymbol{x}_0(\boldsymbol{R})). \tag{A.17}$$

To evaluate this, we invoke Hamilton's equations (A.4) and write

$$\begin{aligned} \nabla_{\boldsymbol{x}} \boldsymbol{\mathcal{F}}(\boldsymbol{R},\boldsymbol{x}) &= -\nabla_{\boldsymbol{x}} \nabla_{\boldsymbol{R}} \Phi(\boldsymbol{R},\boldsymbol{x}) = -\nabla_{\boldsymbol{R}} \nabla_{\boldsymbol{x}} \Phi(\boldsymbol{R},\boldsymbol{x}) \\ &= \nabla_{\boldsymbol{R}} \mathbf{J} \boldsymbol{v}(\boldsymbol{R},\boldsymbol{x}) = \mathbf{J} \nabla_{\boldsymbol{R}} \boldsymbol{v}(\boldsymbol{R},\boldsymbol{x}), \end{aligned} \tag{A.18}$$

Thus, using (A.14)–(A.16),

$$\boldsymbol{F}_1(\boldsymbol{R},\boldsymbol{V}) = \mathbf{M}^{-1}\boldsymbol{V} \cdot \nabla_{\boldsymbol{R}} \boldsymbol{x}_0(\boldsymbol{R}) \cdot \mathbf{J} \nabla_{\boldsymbol{R}} \boldsymbol{v}(\boldsymbol{R}, \boldsymbol{x}_0(\boldsymbol{R})). \tag{A.19}$$

Next, we simplify the last factor by noting that, from the definition (A.6) of $\boldsymbol{x}_0$, the zero-order fast velocity vanishes for all $\boldsymbol{R}$, so its total derivative must also vanish for all $\boldsymbol{R}$:

$$\begin{aligned} 0 &= \nabla_{\boldsymbol{R}} \boldsymbol{v}\,(\boldsymbol{R}, \boldsymbol{x}_0(\boldsymbol{R})) + \nabla_{\boldsymbol{R}} \boldsymbol{x}_0(\boldsymbol{R}) \cdot \nabla_{\boldsymbol{x}} \boldsymbol{v}\,(\boldsymbol{R}, \boldsymbol{x}_0(\boldsymbol{R})) \\ &= \nabla_{\boldsymbol{R}} \boldsymbol{v}\,(\boldsymbol{R}, \boldsymbol{x}_0(\boldsymbol{R})) + \mathbf{M} \nabla_{\boldsymbol{R}} \boldsymbol{x}_0(\boldsymbol{R}), \end{aligned} \tag{A.20}$$

where $\mathbf{M}$ is defined in (A.15). Thus

$$\boldsymbol{F}_1(\boldsymbol{R},\boldsymbol{V}) = -\mathbf{M}^{-1}\boldsymbol{V} \cdot \nabla_{\boldsymbol{R}} \boldsymbol{x}_0(\boldsymbol{R}) \cdot \mathbf{J}\mathbf{M} \nabla_{\boldsymbol{R}} \boldsymbol{x}_0(\boldsymbol{R}), \tag{A.21}$$

where the first dot acts between the vectors in the slow $(\boldsymbol{R}, \boldsymbol{V}, \boldsymbol{F})$ space, and the second dot acts between vectors in fast $(\boldsymbol{x})$ phase space.

Remarkably, the factors $\mathbf{M}$ cancel, even though the vectors and matrices do not commute. To see this, it suffices to write the formulas for one-dimensional fast motion, that is

$$\begin{aligned} \boldsymbol{x} &= \begin{pmatrix} q \\ p \end{pmatrix}, \qquad \mathbf{J} = \begin{pmatrix} 0 & 1 \\ -1 & 0 \end{pmatrix}, \\ \mathbf{M} &= \begin{pmatrix} \partial_r v_r & \partial_p v_r \\ \partial_r v_p & \partial_p v_p \end{pmatrix} = \begin{pmatrix} \Phi_{rp} & \Phi_{pp} \\ -\Phi_{rr} & -\Phi_{rp} \end{pmatrix}, \end{aligned} \tag{A.22}$$

where subscripts denote derivatives. Thus, not writing variables explicitly for the moment, we get from (A.12)

$$\begin{aligned} \boldsymbol{F}_1 = -\frac{1}{\Phi_{rr}\Phi_{pp} - \Phi_{rp}^2} &\left[\begin{pmatrix} -\Phi_{rp} & -\Phi_{pp} \\ \Phi_{rr} & \Phi_{rp} \end{pmatrix} \begin{pmatrix} \boldsymbol{V} \cdot \nabla_{\boldsymbol{R}} q_0 \\ \boldsymbol{V} \cdot \nabla_{\boldsymbol{R}} p_0 \end{pmatrix} \right]^{\mathrm{T}} \\ &\times \begin{pmatrix} 0 & 1 \\ -1 & 0 \end{pmatrix} \begin{pmatrix} \Phi_{rp} & \Phi_{pp} \\ -\Phi_{rr} & -\Phi_{rp} \end{pmatrix} \begin{pmatrix} \nabla_{\boldsymbol{R}} q_0 \\ \nabla_{\boldsymbol{R}} p_0 \end{pmatrix}. \end{aligned} \tag{A.23}$$

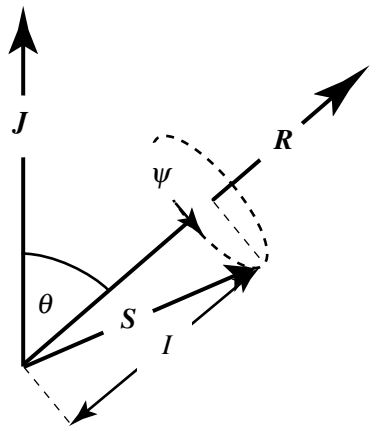

Figure B1. Hamiltonian variables for spin model.

Explicit evaluation of the matrix and vector products gives

$$\boldsymbol{F}_1 = -\boldsymbol{V}\cdot\nabla_{\boldsymbol{R}}q_0\nabla_{\boldsymbol{R}}p_0 + \boldsymbol{V}\cdot\nabla_{\boldsymbol{R}}p_0\nabla_{\boldsymbol{R}}q_0 = \boldsymbol{V}\times(\nabla_{\boldsymbol{R}}q_0\times\nabla_{\boldsymbol{R}}p_0)\,. \tag{A.24}$$

Thus the first-order reaction can be written as a 'magnetic' force,

$$\boldsymbol{F}_1(\boldsymbol{R},\boldsymbol{V}) = \boldsymbol{V}\times\boldsymbol{B}_{\mathrm{g}}(\boldsymbol{R}), \tag{A.25}$$

where $\boldsymbol{B}_{\mathrm{g}}$ is the geometric magnetic field (phase 2-form) that generates the Hannay angle [8, 38]:

$$\boldsymbol{B}_{\mathrm{g}}(\boldsymbol{R}) = \nabla_{\boldsymbol{R}}q_0(\boldsymbol{R})\times\cdot\nabla_{\boldsymbol{R}}p_0(\boldsymbol{R}). \tag{A.26}$$

Here the $\times$ acts between slow gradients $\nabla_{\boldsymbol{R}}$ and the $\cdot$ acts between fast variables $\boldsymbol{q}_0$ and $\boldsymbol{p}_0$. For more general motions, not restricted to the slow manifold, the fast system must be integrable and the 2-form must be averaged over a phase-space torus [38]; but for the special clinging motions we consider here the torus has shrunk to a point, so averaging is unnecessary; indeed the motion could be nonintegrable, so there need not be any tori—the only requirement is an equlibrium state $\boldsymbol{x}_0$.

Appendix B. Hamiltonian form for reduced dynamics (after Littlejohn and Weigert [12])

Equation (2.6) incorporates the constancy of $\boldsymbol{J}$ but is not obviously hamiltonian. To get the dynamics in hamiltonian form, we refer to figure B1 and express (2.1) in the variables

$$R = |\boldsymbol{R}|, \qquad I = \boldsymbol{S}\cdot\boldsymbol{e}_R, \quad \psi. \tag{B.1}$$

Here I is the adiabatic invariant for slowly-varying $\boldsymbol{R}$, and ψ is the (fast) azimuth angle of $\boldsymbol{S}$ relative to $\boldsymbol{R}$. that is

$$\boldsymbol{S} = I\boldsymbol{e}_R + \sqrt{S^2-I^2}(\cos\psi\,\boldsymbol{e}_\theta + \sin\psi\,\boldsymbol{e}_\phi), \tag{B.2}$$

in which $\boldsymbol{e}_\theta$ and $\boldsymbol{e}_\phi$ are the unit polar vectors of the particle position $\boldsymbol{R}$, relative to $\boldsymbol{J}$ which we choose along the z axis, i.e. $\boldsymbol{J} = J\boldsymbol{e}_z$.

Next, we separate the radial and angular parts of the kinetic energy:

$$\boldsymbol{P}\cdot\boldsymbol{P} = P_R^2 + \frac{|\boldsymbol{R}\times\boldsymbol{P}|^2}{R^2} = P_R^2 + \frac{|\boldsymbol{J}-\boldsymbol{S}|^2}{R^2} \tag{B.3}$$

Now

$$|\boldsymbol{J}-\boldsymbol{S}|^2 = J^2 + S^2 - 2\boldsymbol{J}\cdot\boldsymbol{S}, \tag{B.4}$$

and

$$\begin{aligned}\boldsymbol{J}\cdot\boldsymbol{S} &= J\boldsymbol{S}\cdot\boldsymbol{e}_z = J(I\boldsymbol{e}_R\cdot\boldsymbol{e}_z + \sqrt{S^2-I^2}\cos\psi\,\boldsymbol{e}_\theta\cdot\boldsymbol{e}_z)\\ &= J(I\cos\theta - \sqrt{S^2-I^2}\cos\psi\,\sin\theta)\\ &= I^2 - \sqrt{(S^2-I^2)(J^2-I^2)}\cos\psi.\end{aligned} \tag{B.5}$$

In the last line we have used the result, from (2.5),

$$\boldsymbol{J}\cdot\boldsymbol{e}_R = \boldsymbol{S}\cdot\boldsymbol{e}_R, \text{ i.e.} J\cos\theta = I. \tag{B.6}$$

Putting everything together, (3.1) becomes

$$H = \frac{1}{2}\varepsilon P_R^2 + \varepsilon\frac{\left(J^2+S^2-2I^2+2\sqrt{(S^2-I^2)(J^2-I^2)}\cos\psi\right)}{2R^2} + \frac{IR}{\varepsilon}. \tag{B.7}$$

This is the hamiltonian in the canonical variables $\{R, P_R\}$, $\{\psi, I\}$, i.e. two freedoms). J and S are constants. For the evolution of the canonical variables, Hamilton's equations give,

$$\begin{aligned}\dot{R} &= \varepsilon P_R,\\ \ddot{R} &= \varepsilon\dot{P}_R = -I + \varepsilon^2\frac{\left(J^2+S^2-2I^2+2\sqrt{(S^2-I^2)(J^2-I^2)}\cos\psi\right)}{R^3},\end{aligned} \tag{B.8}$$

and

$$\begin{aligned}\dot{\psi} &= \frac{1}{\varepsilon}R - \varepsilon\frac{2I}{R^2} - \varepsilon\frac{I(S^2+J^2-2I^2)\cos\psi}{\sqrt{(S^2-I^2)(J^2-I^2)}\,R^2}\\ \dot{I} &= \varepsilon\frac{\sqrt{(S^2-I^2)(J^2-I^2)}\sin\psi}{R^2}.\end{aligned} \tag{B.9}$$

(The apparent freezing if I starts from the initial value S is illusory, because $I=S$ is a coordinate singularity, easily regularised by considering the dynamics of the angle μ between $\boldsymbol{S}$ and $\boldsymbol{R}$, defined by $I = S\cos\mu$.)

From the solutions, we can determine the remaining unknowns, namely the evolution of the angular variables θ and ϕ of the particle position $\boldsymbol{R}$. θ is given by (B.6), i.e.

$$\cos\theta = \frac{I}{J}, \quad \text{i.e.} \quad \dot{\theta} = -\frac{\dot{I}}{J\sin\theta} = -\frac{\sqrt{S^2-I^2}}{R^2}\sin\psi. \tag{B.10}$$

For ϕ we use

$$\boldsymbol{J}\cdot\boldsymbol{e}_\theta = -J\sin\theta = \boldsymbol{R}\times\boldsymbol{V}\cdot\boldsymbol{e}_\theta + \boldsymbol{S}\cdot\boldsymbol{e}_\theta = -R^2\dot{\phi}\sin\theta + \sqrt{S^2-I^2}\cos\psi, \tag{B.11}$$

so

$$\dot{\phi} = \frac{J}{R^2}\left(1+\sqrt{\frac{S^2-I^2}{J^2-I^2}}\cos\psi\right). \tag{B.12}$$

These hamiltonian evolution equations can be alternatively (and more laboriously) derived by direct transformation of the evolution equations (2.3) and (2.4).

Appendix C. S_2 is the Littlejohn–Weigert (LW) force

Adapted to our notation (including signs and ε scaling), the 'new term' identified in equation (54) of [12] is the term involving ε^3 in the LW slow hamiltonian

$$\begin{aligned} H &= \frac{1}{2}\varepsilon P^2 + \frac{S}{\varepsilon}R + \frac{\varepsilon^3 S}{2R}(\boldsymbol{P}\cdot\nabla_{\boldsymbol{R}}\boldsymbol{e}_R)^2 \\ &= \frac{1}{2}\varepsilon P^2 + \frac{S}{\varepsilon}R + \frac{\varepsilon^3 S}{2R^3}(P^2 - (\boldsymbol{P}\cdot\boldsymbol{e}_R)^2), \end{aligned} \tag{C.1}$$

where we have used

$$(\boldsymbol{P}\cdot\nabla_{\boldsymbol{R}}\boldsymbol{e}_R)^2 = \frac{P^2 - (\boldsymbol{P}\cdot\boldsymbol{e}_R)^2}{R^2} = \frac{P_\perp^2}{R^2}. \tag{C.2}$$

We have ignored the vector potential representing geometric magnetism, because this does not contribute to the lowest-order LW force that we are interested in here, and we have ignored the electric scalar potential because it vanishes for the case considered here, in which $\boldsymbol{S}$ and $\boldsymbol{R}$ are parallel.

To lowest orders in ε, the first Hamilton equation gives

$$\boldsymbol{V} = \varepsilon\boldsymbol{P} + \frac{\varepsilon^3 S}{R^3}\boldsymbol{P}_\perp = \varepsilon\boldsymbol{P} + \frac{\varepsilon^2 S}{R^3}\boldsymbol{V}_\perp. \tag{C.3}$$

The second Hamilton equation gives, also to lowest orders,

$$\dot{\boldsymbol{P}} = -\frac{S}{\varepsilon}\boldsymbol{e}_R + \frac{3\varepsilon S}{2R^4}V^2\boldsymbol{e}_R - \frac{5\varepsilon S}{2R^4}V_\parallel^2\boldsymbol{e}_R + \frac{\varepsilon S}{R^4}V_\parallel\boldsymbol{V}, \tag{C.4}$$

Differentiating (C.3) gives

$$\dot{\boldsymbol{V}} = \varepsilon\dot{\boldsymbol{P}} - \frac{3\varepsilon^2 S}{R^4}V_\parallel\boldsymbol{V}_\perp + \frac{\varepsilon^2 S}{R^3}\dot{\boldsymbol{V}}_\perp. \tag{C.5}$$

Now

$$\begin{aligned} \dot{\boldsymbol{V}}_\perp &= \frac{\mathrm{d}}{\mathrm{d}t}(\boldsymbol{V} - \boldsymbol{V}\cdot\boldsymbol{e}_R\boldsymbol{e}_R) = \dot{\boldsymbol{V}} - \dot{\boldsymbol{V}}\cdot\boldsymbol{e}_R\boldsymbol{e}_R - \boldsymbol{V}\cdot\dot{\boldsymbol{e}}_R\boldsymbol{e}_R - \boldsymbol{V}\cdot\boldsymbol{e}_R\dot{\boldsymbol{e}}_R \\ &= -S\boldsymbol{e}_R + S\boldsymbol{e}_R - \frac{V_\perp^2}{R}\boldsymbol{e}_R - \frac{V_\parallel}{R}\boldsymbol{V}_\perp = -\frac{V_\perp^2}{R}\boldsymbol{e}_R - \frac{V_\parallel}{R}\boldsymbol{V}_\perp, \end{aligned} \tag{C.6}$$

where we have used $\dot{\boldsymbol{e}}_R = \boldsymbol{V}_\perp/R$.

Combining (C.4–6) leads to

$$\dot{\boldsymbol{V}} = -S\boldsymbol{e}_R + \frac{\varepsilon^2 S}{R^4}\left(\frac{1}{2}V_\perp^2\boldsymbol{e}_R - 3V_\parallel\boldsymbol{V}_\perp\right), \tag{C.7}$$

involving exactly the second-order force $-\varepsilon^2\boldsymbol{S}_2$ in (3.13) derived from the general formalism.

Appendix D. Parabolic cylinder asymptotics

We will use the saddle-point method, starting from the definition (formula 9.241.1 of [28])

$$D_p(u) = \sqrt{\frac{2}{\pi}}2^p\exp\left(-\frac{1}{2}\mathrm{i}p\pi + \frac{1}{4}u^2\right)\int_{-\infty}^{\infty}\mathrm{d}t\, t^p\exp(-2t^2 + 2\mathrm{i}tu)\ [\mathrm{Re}\ p > -1] \tag{D.1}$$

This can be used for v in (4.16), in which $p = -\mathrm{i}X^2/4d$. The formula is not valid for u, for which we will use the identity

$$D_{p-1}(u) = \frac{1}{2p}uD_p(u) + \frac{1}{p}\partial_u D_p(u). \tag{D.2}$$

It is convenient to write the integral in the form

$$\int_{-\infty}^{\infty} \mathrm{d}t \exp\{-\Phi(t; X, Z, \delta)\}, \tag{D.3}$$

where

$$\Phi(t; X, Z, \delta) = \mathrm{i}\frac{X^2}{4\delta}\log t + 2t^2 + 2\mathrm{i}\frac{Xt}{\delta}\exp\left(\frac{3}{4}\mathrm{i}\pi\right). \tag{D.4}$$

A short calculation gives the two saddles as

$$\partial_t\Phi(t_\pm) = 0 \Rightarrow t_\pm = \frac{Z \pm R}{4\delta}\exp\left(-\frac{1}{4}\mathrm{i}\pi\right). \tag{D.5}$$

We also need the second derivative

$$\partial_t^2\Phi(t_\pm) = \frac{8}{X^2}R\,(R \mp Z)\,, \tag{D.6}$$

and, most important, the exponents themselves:

$$\Phi(t_\pm) = \frac{\pi X^2}{16\delta} + \frac{\mathrm{i}}{\delta}\left[\frac{1}{4}X^2\log\left(\frac{Z \pm R}{4\sqrt{\delta}}\right) \pm \frac{1}{4}RZ + \frac{1}{8}\left(3Z^2 - R^2\right)\right]. \tag{D.7}$$

We need to know which of the two saddles $t_\pm$ contribute to the integral, in the sense that the integration path in (D.3) can be deformed from the real axis through $t_\pm$, and also which is dominant, in the sense of having the smaller value of $\mathrm{Re}\Phi$. Careful analysis (not given here) of the steepest-descent paths (level curves of $\mathrm{Im}\Phi$ in the t plane) shows that only t_- contributes if $Z < 0$, and both of $t_\pm$ contribute if $Z > 0$. For the dominance, we note that in (D.7) the argument of the logarithm is positive for t_+, and negative for t_- (for both signs of Z). The negative sign contributes an additional term to $\Phi(t_-)$, so

$$\mathrm{Re}\,\Phi(t_+) = \frac{\pi X^2}{16\delta}, \qquad \mathrm{Re}\,\Phi(t_-) = \frac{\pi X^2}{16\delta} - \frac{\pi X^2}{4\delta}, \tag{D.8}$$

showing that the dominant saddle is always t_-.

Now we have all the ingredients for calculating v in (4.16). There is part of the phase that is common to u and v and to $t_\pm$ and therefore does not contribute to $\boldsymbol{S}$ in (4.12). This does not need to be written explicitly, and we denote it by μ. The difference of phase is important for $Z > 0$, when both saddles contribute, and for this we write

$$\Gamma = \mathrm{Im}[\Phi(t_+) - \Phi(t_-)] = \frac{1}{\delta}\left(\frac{1}{4}X^2\log\left(\frac{R+Z}{R-Z}\right) + \frac{1}{2}RZ\right). \tag{D.9}$$

Thus we obtain the asymptotic result

$$v(X, Z, \delta) \approx \frac{\exp(\mathrm{i}\mu)X}{2R}\left(\frac{1}{\sqrt{R+Z}} + \frac{\Theta(Z)}{\sqrt{R-Z}}\exp\left(-\frac{\pi X^2}{4\delta}\right)\exp(-\mathrm{i}\Gamma)\right), \tag{D.10}$$

in which the unit step Θ multiplies the contribution from t_-, which exists only for $Z > 0$. For the calculation of u from (4.16), we use (D.1) and (D.2), realising that in the resulting integral the new factors t are slowly varying and can be replaced by their values at each contributing

saddle. This leads to

$$u(X, Z, \delta) \approx \frac{\exp(\mathrm{i}\mu)X}{2R}\left(\sqrt{R+Z} - \Theta(Z)\exp\left(-\frac{\pi X^2}{4\delta}\right)\sqrt{R-Z}\exp(-\mathrm{i}\Gamma)\right). \qquad \text{(D.11)}$$

The approximate linearized slow manifold (4.19) follows after substituting (D.10) and (D.11) into (4.12).

References

[1] van Kampen N G 1985 Elimination of fast variables *Phys. Rep.* **124** 69–160
[2] Böhm A 2003 *The Geometric Phase in Quantum Systems: Foundations, Mathematical Concepts, and Applications in Molecular and Condensed-Matter Physics* (Berlin, New York: Springer)
[3] Zygelman B 1987 Appearance of gauge potentials in atomic collision physics *Phys. Lett.* A **125** 476–81
[4] MacKay R S 2004 *Lectures on Slow Manifolds in Energy Localization and Transfer* ed T Dauxois (Singapore: World Scientific) pp 149–92
[5] Lorentz E N *et al* 1992 The Slow Manifold – What Is It? *J. Atmos. Sci.* **49** 2449–51
[6] Berry M V 1984 Quantal phase factors accompanying adiabatic changes *Proc. Roy.Soc. Lond.* A **392** 45–57
[7] Chruscinski D and Jamiolkowski A 2004 *Geometric Phases in Classical and Quantum Mechanics* (Boston: Birkhäuser)
[8] Hannay J H 1985 Angle variable anholonomy in adiabatic excursion of an integrable Hamiltonian *J. Phys. A: Math. Gen.* **18** 221–30
[9] Berry M V 1989 *The Quantum Phase, Five Years after in Geometric Phases in Physics* ed A Shapere and F Wilczek (Singapore: World Scientific) pp 7–28
[10] Berry M V and Robbins J M 1993 Classical geometric forces of reaction: an exactly solvable model *Proc. R. Soc. Lond.* A **442** 641–58
[11] Berry M V and Lim R 1990 The Born–Oppenheimer electric gauge force is repulsive near degeneracies *J. Phys. A: Math. Gen.* **23** L655–57
[12] Littlejohn R G and Weigert S 1993 Adiabatic motion of a neutral spinning particle in an inhomogeneous magnetic field *Phys. Rev.* A **48** 924–40
[13] Berry M V and Robbins J M 1993 Chaotic classical and half-classical adiabatic reactions: geometric magnetism and deterministic friction *Proc. Roy. Soc. Lond.* A **442** 659–72
[14] Jarzynski C 1993 Energy diffusion in a chaotic adiabatic billiard gas *Phys. Rev.* E **48** 4340–50
[15] Ramis J and Schäfke R 1996 Gevrey separation of fast and slow variables *Nonlinearity* **9** 353–84
[16] Walton P B 2002 Slow-fast systems pp 175 *PhD Thesis* DAMTP, Cambridge
[17] Lochak P and Meunier C 1988 *Multiphase Averaging for Classical Systems* (New York: Springer)
[18] Gosselin P and Mohrbach H 2008 Appearance of Gauge Fields and Forces beyond the adiabatic approximation arXiv:0810.3640
[19] Gosselin P, Hanssen J and Mohrbach H 2008 Recursive diagonalization of Quantum Hamiltonians to all orders in h *Phys. Rev.* D **77** 085008
[20] Gosselin P, Bérard A and Mohrbach H 2007 Semiclassical diagonalization of quantum Hamiltonian and equations of motion with Berry phase corrections *Eur. Phys. J.* B **58** 137–48
[21] Betz V, Goddard B D and Teufel S 2009 Superadiabatic transitions in quantum molecular dynamics *Proc. R. Soc. Lond.* A **465** 3553–80
[22] Landau L 1932 Zur Theorie der Energieubertragung II *Phys. Soviet Union* **2** 46–51
[23] Majorana E 1932 Atomi orientati in campo magnetico variabile *Nuovo Cimento* **9** 43–50
[24] Zener C 1932 Non-adiabatic crossing of energy levels *Proc. R. Soc. Lond.* A **137** 696–702
[25] Vanneste J 2008 Asymptotics of a slow manifold *SIAM J. Appl. Dynam. Syst.* **7** 1163–90
[26] Aharonov Y and Stern A 1992 Origin of the geometric forces accompanying Berry's geometric potentials *Phys. Rev. Lett.* **92** 3593–97
[27] Marsden J and Weinstein A 1974 Reduction of symplectic manifolds with symmetry *Reps. Math. Phys.* **5** 121–30
[28] Gradshteyn I S and Ryzhik I M 1980 *Table of Integrals, Series and Products* (New York and London: Academic)
[29] Abramowitz M and Stegun I A 1972 *Handbook of Mathematical Functions* (Washington: National Bureau of Standards)
[30] Berry M V 1989 Uniform asymptotic smoothing of Stokes's discontinuities *Proc. R. Soc. Lond.* A **422** 7–21
[31] Berry M V 1990 Histories of adiabatic quantum transitions *Proc. R. Soc. Lond.* A **429** 61–72
[32] Lim R and Berry M V 1991 Superadiabatic tracking for quantum evolution *J. Phys. A: Math. Gen.* **24** 3255–64

[33] Dingle R B 1973 *Asymptotic Expansions: their Derivation and Interpretation* (New York and London: Academic)
[34] Berry M V and Howls C J 1990 Stokes surfaces of diffraction catastrophes with codimension three *Nonlinearity* **3** 281–91
[35] Gelfreich V and Lerman L 2002 Almost invariant elliptic manifold in a singularly perturbed Hamiltonian system *Nonlinearity* **15** 447–57
[36] Brannström N and Gelfreich V 2008 Drift of slow variables in slow-fast Hamiltonian systems *Physica* D **237** 2913–21
[37] Berry M V 2009 Transitionless quantum driving *J. Phys. A: Math. Theor.* **42** 365303 (9pp)
[38] Berry M V 1985 Classical adiabatic angles and quantal adiabatic phase *J. Phys. A: Math. Gen.* **18** 15–27